crystals

Review

Crystal Chemistry and Structural Complexity of the Uranyl Vanadate Minerals and Synthetic Compounds

Ivan V. Kuporev [1], Sophia A. Kalashnikova [1,2] and Vladislav V. Gurzhiy [1,*]

1 Crystallography Department, Institute of Earth Sciences, St. Petersburg State University, University Emb. 7/9, St. Petersburg 199034, Russia; st054910@student.spbu.ru (I.V.K.); st055416@student.spbu.ru (S.A.K.)
2 Laboratory of Nature-Inspired Technologies and Environmental Safety of the Arctic, Nanomaterials Research Centre, Kola Science Center, Russian Academy of Sciences, Fersmana Str., 14, Apatity 189209, Russia
* Correspondence: vladislav.gurzhiy@spbu.ru or vladgeo17@mail.ru

Abstract: This paper reviews perhaps one of the most enigmatic groups of secondary uranium minerals. The number of uranyl vanadate mineral species does not reach even 20, and they do not display a large range of structural diversity, but those natural phases form rather massive deposits that can be mined as uranium ores. The number of synthetic uranyl vanadates is three times higher than natural phases, and most of them were obtained using hydrothermal and solid-state techniques. Diversity is also evident in their structural parts. The majority of synthetic compounds, both pure inorganic or organically templated, have their structures based upon mineral-like substructural units of francevillite, uranophane, U_3O_8, and other common topological types, and not even one compound among 57 studied was obtained from simple aqueous solutions at room temperature. This allows us to assume that even under natural conditions, elevated temperatures are required for the formation of isotypic uranyl vanadate minerals, especially in the case of industrially developed thick strata. The structural complexity parameters for natural uranyl vanadates directly depend on the unit cell volume. Keeping in mind that all minerals possess layered structural architecture, it means that structural complexity increases with the increase in the interlayer spacing, which, in turn, depends on the size of cations or water–cationic complexes arranged in the interlayer space. This tendency similarly works for organic molecules, which are incorporated into the uranyl vanadate frameworks. It can also be concluded that the architecture of the uranyl vanadate substructural units defines the complexity of the entire crystal structure.

Keywords: uranyl; vanadate; mineral; crystal structure; topology; structural complexity

check for updates

Academic Editor: José L. Arias

Received: 10 December 2024
Revised: 27 December 2024
Accepted: 27 December 2024
Published: 30 December 2024

Citation: Kuporev, I.V.; Kalashnikova, S.A.; Gurzhiy, V.V. Crystal Chemistry and Structural Complexity of the Uranyl Vanadate Minerals and Synthetic Compounds. *Crystals* **2025**, *15*, 43. https://doi.org/10.3390/cryst15010043

1. Introduction

Uranyl vanadates are perhaps one of the most enigmatic groups of secondary uranium minerals. On the one hand, they form rather massive deposits that can be mined as uranium ores [1–3]; on the other hand, the number of mineral species does not reach 20, most of which were discovered in the early to mid-XXth century and remain incompletely studied to this day [4–6]. The same is true for structural diversity. Almost all reliably studied natural uranyl vanadates are members of the carnotite group with a U:V ratio of 1:1. The only exceptions are two recently discovered uranyl sulfate–vanadates, in which vanadium is found in subordinate amounts (U:S:V = 4:4:1). This might come from the natural formation conditions. Uranium and V are generally not concentrated in the same geochemical environments with the exception of breccia pipes and similar environments in continental basins where redox reactions with organic material precipitate and bind U and V, which allow for trace concentrations of U and V in the groundwater to be locally enriched to ore-grade. A relatively representative group of synthetic compounds is limited by rather uniform conditions for synthesis pathways. At the same time, among the known synthetic compounds, there are quite a few isostructural analogs, which impose limitations on the comparison of compounds of this group.

Herein, we present a review of a family of natural and synthetic uranyl vanadate compounds, which is a continuation of a series of review papers on the crystal chemistry of various groups of uranyl minerals and their synthetic analogs [7–9]. There are no previous systematic studies of uranyl vanadate compounds, so current work includes not only structural and crystal–chemical characterization but also topological analysis and particularities of synthetic protocols for all known to date uranyl vanadate compounds. Despite the limitations mentioned above, several groups were identified among the total number of compounds, the structural features of which allowed us to discuss some crystal chemical trends. Calculation of the structural complexity parameters helped to generalize an idea about the stability and principles of uranyl–vanadate structural complexes formation in various media.

2. Materials and Methods

2.1. Structural Data

For the current review, all structural data deposited in the Inorganic Crystal Structure Database (ICSD; version 5.3.0; release February 2024) and the Cambridge Structural Database (CCDC; WebCSD version; October 2024) were selected and supplemented by the data reported in the most recent publications. Chemical formulae, mineral names, and crystallographic parameters for all uranyl vanadates of natural and synthetic origin are listed in Tables 1–3. In addition, Table 1 contains information on the uranyl vanadate minerals with yet undefined crystal structures listed in the IMA Database of Mineral Properties [10].

2.2. Graphical Representation and Anion Topologies

The crystal structures of uranyl vanadate compounds of both natural and synthetic origin discussed in this review are built by the layered and framework motifs constructed by the linkage of U- and V-centered coordination polyhedra. Uranium atoms make two short $U^{6+} \equiv O^{2-}$ bonds to form approximately linear UO_2^{2+} uranyl cations, which are surrounded in the equatorial plane by other four, five, or six O atoms; this results in the formation of a tetra-, penta- or hexagonal bipyramids as coordination polyhedra of U(VI) atoms. Vanadium atoms are coordinated by four or five O atoms to form tetrahedral or tetragonal pyramidal coordination geometry. Such coordination types are very close to those described for the family of uranyl molybdate compounds [9]. However, the latter also has a distorted octahedral coordination, which is technically close to the tetragonal pyramidal coordination if one of the octahedral apical ligands moves away from the central Mo atom (c.a. 2.5 Å). It should be mentioned that for uranyl vanadate structures, it is common to contain pyrovanadate groups or dimers of edge-shared tetragonal vanadate pyramids.

The topology of the uranyl vanadate building blocks can be represented in different ways depending on the U–V unit dimension and the interpolyhedral connection between the uranyl and vanadate coordination polyhedra (Figure 1). The anion topology approach introduced by Burns et al. [11,12] is used for the description of the uranyl vanadate crystal structures that are based on layers with edge-sharing linkage of U-centered polyhedra. The theory of nodal representation, which was suggested by Hawthorne [13] and then effectively applied by Krivovichev [14–16], is used to describe layers and frameworks with vertex-sharing linkage. Topological analysis utilizing natural tiling methods for 3D cation networks can effectively characterize frameworks [17], including heteropolyhedral ones [18,19].

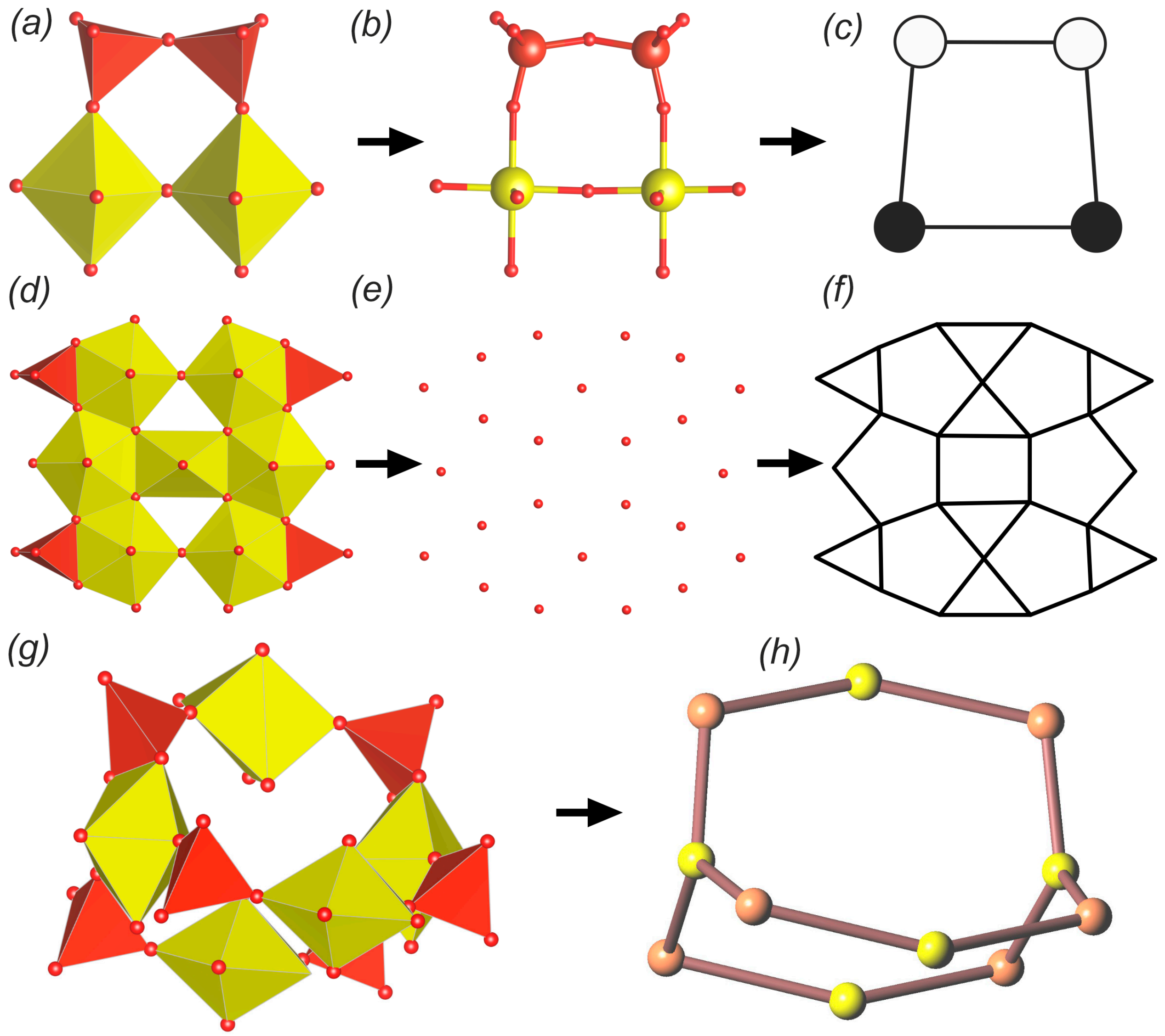

Figure 1. Various approaches of topology representation. Vertex-sharing linkage of uranyl bipyramids with and $(VO_4)^{3-}$ tetrahedra in polyhedral (**a**), ball-and-stick (**b**) representations, and respective black-and-white graph (**c**). Edge-sharing interpolyhedral resulting in a dense uranyl–vanadate layer formation (**d**), O atoms that are involved in linkage with more than one cation (**e**), and the resulted anion topology built on them (**f**). Fragment of a heteropolyhedral framework (**g**) and its 3D net representation (**h**). Legend: U-bearing coordination polyhedra = yellow; U atoms = yellow; V-centered tetrahedra = orange; V atoms = orange; O atoms = red; black nodes = U atoms, white nodes = V atoms; see Section 2.2 for details.

The black-and-white graph has the index *cc*D–U:V–#, where *cc* corresponds to the cation-centered type of the interpolyhedral linkage; D indicates dimensionality (0—finite clusters; 1—chains; 2—sheets, and 3—framework) and U:V ratio, and #—registration number of the unit. The anion topology of the U-bearing sheets has the ring symbol, $p_1{}^{r1}p_2{}^{r2}\ldots$, where *p* is the number of vertices in a topological cycle, and *r* is the number of particular cycles in the reduced fragment of the uranyl vanadate layer. Face symbols can be used to represent tiles that make up a net. They contain information in the following form: $[A^a.B^b\ldots]$, indicating that there are *a* faces that are *A*-rings and *b* faces that are *B*-rings. Since the natural tiling may include tiles of different compositions, a tile signature is used that contains information about the number and ratio of tiles. Such signatures can be calculated using the ToposPro version 5.5.2.2 software package [20]. To determine natural tilings of the heteropolyhedral frameworks, the structures were preliminarily simplified by removing additional cations located in the cavities and contracting all oxygen atoms toward U and V atoms (in cases containing P and I groups, the corresponding atoms were also retained). For the resulting simplified frameworks, possible primitive proper tilings were identified. When multiple tilings were possible, the natural tiling was always selected. The maximum ring size setting varied depending on the specific structure and computational limitations. Simplification of structures and calculation of tilings was carried out in the ADS module.

2.3. Complexity Calculations

Structural complexity calculation is a mathematical approach for numerically characterizing various structural units (U-containing complex, interstitial cations, hydration state, etc.) and assessing their role in terms of information content in the organization and influence on the formation of the structural architecture of a crystalline compound as a whole. This approach was proposed fifteen years ago by Krivovichev [14–16,21,22] and has been successfully used in a number of recent papers (e.g., [7–9,23–29]). It is based on the Shannon information content calculations of per atom (I_G) and per unit cell ($I_{G,total}$) using the following equations:

$$I_G = -\sum_{i=1}^{k} p_i \log_2 pi \qquad \text{(bits/atom)} \tag{1}$$

$$I_{G,total} = -v\, I_G = -v\sum_{i=1}^{k} p_i \log_2 pi \quad \text{(bits/cell)} \tag{2}$$

where k is the number of different crystallographic orbits (independent sites) in the structure, and p_i is the random choice probability for an atom from the i-th crystallographic orbit, that is

$$p_i = m_i/v \tag{3}$$

Direct matching of structural complexity parameters is possible only for compounds with the same or very similar chemical composition (e.g., polymorphs), whereas even minor changes (e.g., in the nature of interstitial ions and molecules, hydration state, etc.) can significantly affect the final complexity values. Therefore, it is necessary to compare the values carefully. Complexity parameters for the structures have been determined using ToposPro software [20]. The complexity of the partially disordered crystal structures was taken into account in favor of the main component. In addition, the positions of all hydrogen atoms were assigned manually in cases where such data were not provided in the original records. This placement was performed with careful consideration of the hydrogen bond network, adhering to the usual ranges of bond lengths and angles in the D-H A system (where D is the donor atom and A is the acceptor atom, both typically oxygen).

Table 1. Crystallographic characteristics and structural complexity parameters of natural uranyl vanadates.

No.	Chemical Formula	Mineral Name	Sp. Gr.	*a*, Å/ α, °	*b*, Å/ β, °	*c*, Å/ γ, °	Structural Complexity Parameters, Bits per Atom/Bits per Unit Cell		Ref.
			Layers				**U-Bearing Unit**	**Entire Structure**	
	Francevillite Topology, $5^1 4^1 3^1$								
1	$Ba_{0.96}Pb_{0.04}(UO_2)_2(V_2O_8)(H_2O)_5$	Francevillite	*Pcan*	10.419/90	8.510/90	16.763/90	3.000/192.000	4.063/520	[30–32]
2	$Pb_4(UO_2)_2)(V_2O_8)(H_2O)_5$	Curienite	*Pcan*	10.419/90	8.494/90	16.405/90	3.000/192.000	3.986/494.32	[32–34]
3	$K_2(UO_2)_2(VO_4)_2(H_2O)_3$	Carnotite	$P2_1/c$	10.47/90	8.41/104.2	6.91/90	3.000/96.000	3.17/114.117	[32,35,36]
4	$Cs_2(UO_2)_2(VO_4)_2(H_2O)$	Margaritasite	$P2_1/a$	10.514(3)/90	8.425(3)/106.01	7.252(5)/90	3.000/96.000	3.322/132.880	[37,38]
5	$Cu[(UO_2)(VO_4)](OH)(H_2O)_3$	Sengierite	$P2_1/a$	10.599/90	8.093/103.42	10.085/90	3.000/96.000	4.322/345.754	[39–41]
6	$Ca[(UO_2)_2(VO_4)]_2(H_2O)_{5\text{-}8}$	Tyuyamunite	*mmm*	10.63/90	8.36/90	20.40/90			[42–44]
7	$Ca[(UO_2)_2(VO_4)_2](H_2O)_5$	Metatyuyamunite	*Pbcn*	8.575(3)/90	10.584(3)/90	16.856(5)/90	3.000/192.000	4.146/563.895	[32,44,45]
8	$Na_{2.28}[(UO_2)_{1.84}(V_2O_8)](H_2O)_{3.85}$	Strelkinite	*Pnmm* or *Pnm2*	10.64(2)/90	8.36(2)/90	32.72(2)/90			[46]
9	$K_2[(UO_2)_2V_2O_8](H_2O)$	Vandermeerscheite	$P2_1/n$	8.292(2)/90	8.251(3)/110.84(3)	10.188(3)/90	3.000/96.000	3.459/152.215	[47]
10	$Al[(UO_2)_2(VO_4)_2](OH)(H_2O)_{8.5}$	Vanuralite	$P2_1/n$	10.4637(10)/90	8.4700(5)/102.821(9)	20.527(2)/90	4.000/256.000	5.426/933.318	[48,49]
11	$Ni[(UO_2)_2(V_2O_8)](H_2O)_4$	Metavanuralite	Triclinic	10.46(3)/75.88(33)	8.44(3)/102.83(33)	10.43(3)/90.00(33)			[50]
12	$Sr[(UO_2)_2(V_2O_8)](H_2O)_5$	Finchite	*Pcan*	10.363(6)/90	8.498(5)/90	16.250(9)/90	3.000/192.000	4.063/520.000	[51]
	$8^1 5^3 4^3 3^8$								
13	$K_5[(UO_2)_4(SO_4)_4(VO_5)](H_2O_4)]$	Mathesiusite	$P4/n$	14.970/90	14.970/90	8.817/90	3.353/254.842	3.890/427.95	[52]
14	$(NH_4)_{5.84}(UO_2)_4(SO_4)_4(VO_5)(H_2O)_4$	Ammoniomathesiusite	$P4/n$	14.9405(9)/90	14.9405(9)/90	7.1020(5)/90	3.353/254.842	4.309/646.323	[53]
	Unknown								
15	$Mn[(UO_2)_2(VO_4,PO_4)_2](H_2O)_{4\text{-}10}$	Fritzscheite							[54]
16	$Ca(UO_2)_2(V_{10}O_{28})\cdot 16H_2O$	Rauvite							[55]
17	$(UO_2)_2(V_6O_{17})\cdot 15H_2O$	Uvanite							[56]

Table 2. Crystallographic characteristics and structural complexity parameters of synthetic inorganic uranyl vanadates.

No.	Chemical Formula	Sp. Gr.	a, Å/ α, °	b, Å/ β, °	c, Å/ γ, °	Syn. *	Structural Complexity Parameters, Bits per Atom/Bits per Unit Cell		Ref.
			Layers				**U-Bearing Unit**	**Entire Structure**	
	Francevillite topology, $5^14^13^1$								
18	$Na[(UO_2)(VO_4)]$	$P2_1/c$	6.0205(1)/90	8.2844(2)/97.644(2)	10.5011(2)/90	SS [1000]	3.000/96.000	3.17/114.117	[57]
19	$Na[(UO_2)(VO_4)]\cdot H_2O$	$P2_1/c$	7.722(2)/90	8.512(1)/113.18(3)	10.480(4)/90	SS/N2 [120]	3.000/96.000	3.44/114.477	[57]
20	$Na[(UO_2)(VO_4)]\cdot 2H_2O$	$P2_1/n$	16.2399(5)/90	8.2844(2)/97.644(2)	10.5011(2)	HT [130]	4.000/256.000	4.907/588.827	[57]
21	$Cs_2(UO_2)_2(V_2O_8)$	$P2_1/a$	10.521(2)/90	8.437(9)/106.08(1)	7.308(3)/90	SS [700]	3.000/96.000	3.17/114.117	[58]
22	$Ag_2(UO_2)_2(V_2O_8)$	$P2_1/c$	5.8952(2)/90	8.3541(2)/100.56(1)	10.4142(3)/90	HT [220]	3.000/96.000	3.17/114.117	[59]
23	$(H_3O)(UO_2)(VO_4)$	$P2_1/c$	6.9918(10)/90	8.2655(12)/107.014(4)	10.5062(15)/90	HT [200]	3.000/96.000	3.585/172.078	[60]
24	$La_2[(UO_2)_2V_2O_8]_3(H_2O)_6$	$P2_1/c$	7.9090(9)/90	24.2830(19)/116.498(8)	10.4411(15)/90	HT [190]	3.000/96.000	5.17/744.469	[61]
25	$Nd_2[(UO_2)_2V_2O_8]_3(H_2O)_{22}$	$P2_1/c$	9.6530(6)/90	10.5242(6)/103.30(3)	26.3024(15)/90	HT [190]	4.585/440.156	5.644/1128.771	[61]
26	$Y_2[(UO_2)_2V_2O_8]_3(H_2O)_{20}$	$P2_1/c$	9.3464(3)/90	10.5212(3)/102.90(10)	25.2094(7)/90	HT [190]	4.585/440.156	5.833/1329.899	[61]
27	$Nd(UO_2)_3(VO_4)_3(H_2O)_{11}$	$P2_1/n$	9.6260(16)/90	10.5128(18)/98.425(4)	24.793(4)/90	HT [200]	4.585/440.156	5.615/1100.483	[60]
28	$Eu(UO_2)_3(VO_4)_3(H_2O)_{10}$	$P2_1/n$	9.537(2)/90	10.527(2)/98.487(7)	24.862(5)/90	HT [200]	4.585/440.156	5.615/1100.483	[60]
29	$La_2[(UO_2)_2V_2O_8]_3(H_2O)_{20}$	$P2_1/c$	9.8269(3)/90	24.8017(6)/105.88(2)	10.5986(3)/90	HT [190]	4.585/440.156	5.524/1016.335	[61]
	β-U_3O_8-sheet topology, $5^44^23^4$								
30	$Cs_7(UO_2)_8(VO_4)_2ClO_8$	*Pmmn*	21.458(3)/90	11.773(2)/90	7.495(1)/90	SS [750]	3.891/334.659	4.124/412.386	[62]
31	$Rb_7(UO_2)_8(VO_4)_2ClO_8$	*Pmcn*	21.427(5)/90	11.814(3)/90	14.203(3)/90	SS [600]	4.589/789.318	4.804/960.771	[62]
	Fragment of β-U_3O_8, $5^44^33^4$								
32	$Na_6(UO_2)_5(VO_4)_2O_5$	$P2_1/c$	12.584(1)/90	24.360(2)/100.61(1)	7.050(1)/90	Flx [775]	4.907/588.827	5.17/744.469	[63]
33	β-$Rb_6(UO_2)_5(VO_4)_2O_5$	$P2_1/n$	7.164(9)/90	14.079(2)/90.23(1)	24.965(4)/90	SS [1200]	4.907/588.827	5.198/748.469	[64]
34	$K_6(UO_2)_5(VO_4)_2O_5$	$P2_1/c$	6.856(1)/90	24.797(3)/98.79(8)	7.135(1)/90	SS [775]	3.974/238.413	4.225/304.235	[63]
	Fragment of α-U_3O_8, $5^54^23^4$								
35	α-$Rb_6(UO_2)_5(VO_4)_2O_5$	$C2/c$	24.887(8)/90	7.099(2)/103.92(1)	14.376(4)/90	SS [650]	3.974/238.413	4.225/304.235	[64]
	$6^14^23^2$								
36	$Cs(UO_2)(VO_3)_3$	$P2_1$/a	11.904(2)/90	6.8321(6)/106.989(5)	12.095(2)/90	SS [300–650]	3.907/234.413	4/256	[65]
	cc2-1:1-19								
37	$Cs_4[(UO_2)_2(V_2O_7)O_2]$	*Pmmn*	8.483(15)/90	13.426(2)/90	7.137(13)/90	SS [980]	2.676/90.974	3.154/132.477	[66]
	Uranophane topology								
38	$Sr_3(UO_2)(V_2O_7)_2$	*P*-1	6.891(3)/85.201(4)	7.171(3)/78.003(4)	14.696(6)/89.188(4)	Flx [870]	3.585/86.039	4.585/220.078	[67]
39	$[La(UO_2)V_2O_7][(UO_2)(VO_4)]$	$P2_12_12_1$	6.9470(2)/90	7.0934(2)/90	25.7464(6)/90	SS [870]	4.322/345.754	4.392/368.955	[68]

Table 2. *Cont.*

No.	Chemical Formula	Sp. Gr.	*a*, Å/ α, °	*b*, Å/ β, °	*c*, Å/ γ, °	Syn. *	Structural Complexity Parameters, Bits per Atom/Bits per Unit Cell		Ref.
			Layers				**U-Bearing Unit**	**Entire Structure**	
				Framework					
	$[3^4\ 6^2] + [3^4\ 4^2\ 6^2]$								
40	$(UO_2)(VO_3)$	*Pbcm*	4.1231(1)/90	12.3641(1)/90	7.2071(1)/90	SQT [700]	2.522/70.606	2.522/70.606	[58]
	$[8^3] + [3^4\ 8^2] + [3^4\ 4^4\ 8\ 10^2]$								
41	$(UO_2)_3(VO_4)_2(H_2O)_5$	*Cmcm*	17.978(2)/90	13.561(2)/90	7.163(1)/90	HT [60]	3.059/110.117	3.599/223.16	[69]
42	$(UO_2)_3(VO_4)_2(H_2O)_3$	*Pnma*	27.108(3)/90	17.7466(17)/90	7.1288(7)	HT [200]	4.641/816.86	5.253/1365.816	[60]
	$[3^2\ 7^2] + [3^2\ 4^2\ 6\ 7^2]$								
43	$(UO_2)_2(V_2O_7)$	*P*2₁/*c*	5.6492(1)/90	13.1841(2)/119.745(1)	7.2844(1)/90	SS [600–650]	2.974/89.207	2.974/89.207	[70]
	$2[8^3] + [8^4]$								
44	$Ca(UO_2)(V_2O_7)$	*Pmn*2₁	7.1774(18)/90	6.7753(17)/90	8.308(2)/90	Flx [870]	3.252/78.039	3.393/88.211	[67]
	$[6^2\ 8^2] + [8^2\ 10^2]$								
45	$Sr(UO_2)(V_2O_7)$	*Pnma*	13.4816(11)/90	7.3218(6)/90	8.4886(7)/90	Flx [870]	3.252/156.078	3.393/176.423	[67]
46	$Pb(UO_2)(V_2O_7)$	*P*2₁/*n*	6.9212(9)/90	9.6523(13)/91.74(1)	11.7881(16)/90	SS [680]	3.585/172.078	3.7/192.423	[71]
	$2[5^2\ 8^2] + [3^4\ 8^2]$								
47	$Li_2(UO_2)_3(VO_4)_2O$	*I*4₁*/amd*	7.3303(5)/90	7.3303(5)/90	24.653(3)/90	SS [1000]	2.822/112.877	3.005/132.215	[72]
	$4[5^2\ 8^2] + 2[3^4\ 8^2] + [5^8]$								
48	$Na(UO_2)_4(VO_4)_3$	*I*4₁*/amd*	7.227(4)/90	7.227(4)/90	34.079(4)/90	SS [920]	3.199/172.764	3.341/193.763	[73]
	$8[5^2\ 8^2] + 2[3^4\ 8^2] + [5^8]$								
49	$Ag_3(UO_2)_7(VO_4)_5O$	*P*-4*m*2	7.2373(3)/90	7.2373(3)/90	14.7973(15)/90	SS [900]	4.023/189.066	4.104/209.294	[74]
50	$Li_3(UO_2)_7(VO_4)_5O$	*P*-4*m*2	7.2794(9)/90	7.2794(9)/90	14.514(4)/90	SS [950]	4.023/189.066	4.182/213.294	[74]
	$2[4^3] + [3^4\ 8^2] + [3^{36}\ 4^{22}\ 8^4\ 12^2]$								
51	$Eu_2(UO_2)_{12}(VO_4)_{10}(H_2O)_{24}$	*P*1	11.203(2)/71.622(5)	13.368(2)/72.296(5)	15.644(3)/77.051(5)	HT [200]	6.524/600.168	7.476/1330.681	[60]
	$[4^2\ 10^2] + [3^4\ 8^4\ 10^2]$								
52	$Cs_2[UO_2(VO_2)_2(PO_4)_2](H_2O)_{0.59}$	*Cmc*2₁	20.7116(14)/90	6.8564(5)/90	10.5497(7)/90	HT [190]	3.406/129.421	3.641/160.215	[75]
	$2[3^2\ 4^2] + [4^2\ 8^2] + [8^2\ 10^2] + [3^4\ 4^{14}\ 10^2]$								
53	$K_{3.48}[(UO_2)H_{1.52}(VO)_4(PO_4)_5]$	*Immm*	7.3803(7)/90	9.1577(8)/90	17.0898(16)/90	HT [190]	3.426/147.329	3.505/154.215	[76]
	$2[3^4\ 10^2] + [3^8\ 4^4\ 6^2\ 10^2]$								
54	$K_2[(UO_2)_2(VO)_2(IO_6)_2O](H_2O)$	*Pba*2	9.984(2)/90	16.763(3)/90	4.977(1)/90	HT [120]	3.684/184.193	3.974/238.413	[77]

* Synthesis data. SS[T] corresponds to solid-state synthesis at maximum reported temperature T (°C). SS/N2[T] corresponds to the solid-state topotactic phase transition under the N_2 flow at reported T (°C). HT[T] corresponds to hydrothermal synthesis at maximum reported temperature T (°C). Flx means usage of molten flux in a synthesis. SQT is the Sealed Quartz Tube method.

Table 3. Crystallographic characteristics and structural complexity parameters of synthetic organically-templated uranyl vanadates.

No.	Chemical Formula	Sp. Gr.	*a*, Å/ α, °	*b*, Å/ β, °	*c*, Å/ γ, °	Syn. *	Structural Complexity Parameters, Bits per Atom/Bits per Unit Cell		Ref.
				Layers			**U-Bearing Unit**	**Entire Structure**	
	Francevillite topology, $5^1 4^1 3^1$								
55	$(NH_4)_2[(UO_2)_2V_2O_8]$	$P2_1/c$	6.894(2)/90	8.384(3)/106.066(5)	10.473(4)/90	HT [180]	3.000/96.000	3.700/192.423	[78]
56	$(H_2DMPIP)[(UO_2)_2V_2O_8]$	$P2_1/b$	9.3146(14)/90	8.6174(13)/90	10.5246(2)/114.776(2)	HT [180]	3.000/96.000	3.907/234.413	[78]
57	$(H_2EN)[(UO_2)_2V_2O_8]$	$P2_1/a$	13.9816(6)/90	8.6166/90	10.4237/93.1251	HT [180]	4.000/256.000	4.524/416.168	[78]
58	$(H_2DAP)[(UO_2)_2V_2O_8]$	*Pmcn*	14.7363(8)/90	8.6379/90	10.429/90	HT [180]	3.000/192.000	3.907/468.827	[78]
	Uranophane topology								
59	$(H_2PIP)[(UO_2)_2(VO_4)_2]\cdot 0.8H_2O$	$C2/m$	15.619(2)/90	7.1802(8)/101.500(2)	6.9157(8)/90	HT [180]	2.750/44.000	3.507/105.207	[78]
60	$(H_2DABCO)[(UO_2)_2(VO4)_2]$	$C2/m$	17.440(2)/90	7.1904(9)/98.196(2)	6.8990(8)/90	HT [180]	2.750/44.000	3.500/112.000	[78]
					Framework				
	Pillared uranophane sheets-I								
61	$(C_5NH_6)_2\{[(UO_2)(H_2O)][(UO_2)(VO_4)]_4\}\cdot H_2O$	*P*1	9.6981(3)/117.194(1)	9.9966(2)/113.551(1)	10.5523(2)/92.216(1)	HT [180]	5.170/186.117	5.977/376.569	[79]
	Pillared uranophane sheets-II								
62	$(C_7N_2H_{22})\{[(UO_2)(H_2O)][(UO_2)(VO_4)]_4\}$	$Cmc2_1$	15.9505(6)/90	14.1889(6)/90	13.7168(5)/90	HT [180]	4.281/308.235	5.287/697.86	[80]
63	$(C_3N_2H_{12})\{[(UO_2)(H_2O)][(UO_2)(VO_4)]_4\}\cdot$H2O	$Cmc2_1$	15.2754(2)/90	14.1374(2)/90	13.6609(2)/90	HT [180]	4.281/308.235	5.103/602.152	[80]
64	$(C_2NH_8)_2\{[(UO_2)(H_2O)][(UO_2)(VO_4)]_4\}\cdot H_2O$	$Cmc2_1$	15.6276/90	14.1341/90	13.604/90	HT [180]	4.281/308.235	5.260/704.856	[79]
65	$(C_5N_2H_{16})\{[(UO_2)(H_2O)][(UO_2)(VO_4)]_4\}$	$Cmc2_1$	15.7246(7)/90	14.1208(5)/90	13.5697(5)/90	HT [180]	4.281/308.235	5.137/606.152	[80]
66	$(C_6N_2H_{20})\{[(UO_2)(H_2O)][(UO_2)(VO_4)]_4\}$	$Cmc2_1$	15.6926(5)/90	14.2108(3)/90	13.7003(3)/90	HT [180]	4.281/308.235	5.177/631.55	[80]
67	$(C_4N_2H_{14})\{[(UO_2)(H_2O)][(UO_2)(VO_4)]_4\}\cdot 2H_2O$	$Cmc2_1$	15.558(1)/90	14.1876(9)/90	13.6903(9)/90	HT [180]	4.281/308.235	5.14/616.827	[80]
	Pillared uranophane sheets-III								
68	$(C_6NH_{14})\{[(UO_2)(H_2O)_2][(UO_2)(VO_4)]_3\}\cdot H_2O$	*P*-1	9.8273(6)/98.461(3)	11.0294(7)/96.437(3)	12.7506(8)	HT [180]	4.858/281.763	5.672/578.587	[79]
69	$(C_4NH_{12})\{[(UO_2)(H_2O)][(UO_2)(VO_4)]_3\}$	$P2_1$/m	9.8048(4)/90	17.4567(8)/106.103(2)	15.4820(6)/90	HT [180]	4.956/564.949	5.500/891.056	[79]
	Pillared uranophane sheets-IV								
70	$(C_2NH_8)\{[(UO_2)(H_2O)_2][(UO_2)(VO_4)]_3\}\cdot H_2O$	$P2_1$/n	10.2312(4)/90	13.5661(7)/96.966(2)	17.5291(7)/90	HT [180]	4.858/563.526	5.555/1044.263	[79]
71	$(C_3NH_{10})\{[(UO_2)(H_2O)_2][(UO_2)(VO_4)]_3\}\cdot H_2O$	$P2_1$/n	10.35070(10)/90	13.6500(2)/97.5510(1)	17.3035(2)/90	HT [180]	4.858/563.526	5.585/1072.313	[79]
72	$(N(CH_3)_4)\{[(UO_2)(H_2O)_2][(UO_2)(VO_4)]_3\}\cdot H_2O$	*Pbca*	17.1819(2)/90	13.6931(1)/90	21.4826(2)/90	HT [180]	4.858/1127.052	5.728/2428.638	[79]
					Nanoclusters				
73	$(EMIm)_8[(UO_2)_2(V_{16}O_{46})]\cdot 4H_2O$	$C2/c$	23.656(4)/90	14.981(2)/112.886(2)	27.970(4)/90	Aq/IL	5.087/691.895	6.805/3035.201	[81]
74	$(EMIm)_{15}Na_5[(UO_2)_{20}(V_2O_7)_{10}(SO_4)_{10}]\cdot 80H_2O$	*Pccn*	32.023(3)/90	27.232(3)/90	28.774(3)/90	Aq/IL	6.644/5315.085	7.209/8535.993	[81]

* Synthesis data. SS[T] corresponds to solid-state synthesis at maximum reported temperature T (°C). HT[T] corresponds to hydrothermal synthesis at maximum reported temperature T (°C). Flx means usage of molten flux in a synthesis. SQT is the Sealed Quartz Tube method. Aq/IL is deciphered as synthesis at the boundary of aqueous and ionic liquid solutions at room temperature.

3. Results and Discussion

3.1. Uranyl Vanadate Minerals

Uranyl vanadate minerals (Table 1) are common in bedded or roll-front deposits (the Burro mine, Slick Rock district, San Miguel County, Colorado, USA, for example) [53,82]. Uranyl vanadates are formed through the oxidation of ores containing both uranium and vanadium, primarily through the action of groundwater, and usually form in sandstones [52,53]. The minerals are commonly found in association with other uranyl vanadates, uranyl phosphates, uranyl sulfates, vanadates, uraninite, quartz, gypsum, etc.

One of the greatest known concentrations of uranyl vanadate deposits, particularly carnotite, is in the Western United States, especially in the Colorado Plateau area [83]. A significant number of discoveries belong to the Mounana Mine in Gabon, and some minerals were also found at Svornost Mine, Czech Republic [52]. The crystals of uranyl vanadates are usually met in sedimentary rocks, especially in sandstone. Uranyl vanadates typically contain vanadium in the +5 oxidation state (V^{5+}) and hexavalent uranium (U^{6+}). The minerals usually coexist as radial aggregates, plates, and microcrystalline powder on other crystals [33,48,84].

Today, seventeen uranyl vanadate minerals are known, but their level of study leaves much to be desired. The earliest discovery records of uranyl vanadate minerals date back to the second half of the XIX century. Two works can be mentioned here: Breithaupt in 1865 [54] and Friedel and Cumenge in 1899 [35]. The minerals described were fritzscheite and carnotite, respectively, which were found as yellow powder and powdery masses. The type localities for the aforementioned minerals are Georg Wagsfort Mine (Saxony, Germany) and Rajah Mine (Montrose County, CO, USA).

The first findings of uranyl vanadates in the XX century were in 1912 at the Tyuya-Muyun Cu-V-U deposit (Kyrgyzstan) [42], in 1914 [56], and in 1922 [55], at the Colorado Plateau (Emery County, UT, USA). Those were tyuyamunite, uvanite, and rauvite minerals, respectively. It is of interest that all three minerals have not been fully studied. At least their crystal structures are not yet determined. However, the one for tyuyamunite is assumed by analogy with other minerals of the carnotite group.

In the middle of the XX century, largely due to work on the Manhattan Project and also within the framework of the development of Soviet nuclear energy, a large group of secondary uranium minerals were discovered, and uranyl vanadates were not an exception. Thus, the mineral sengierite was reported in 1949 from the well-known Haut-Katanga province in DR Congo [39]. In 1953, calcium uranyl vanadate metatyuamunite was discovered [44]. It was found again in the Colorado Plateau in the USA as radial aggregates and powdery crystals. Mineral francevillite, which is named after its type locality in Mounana Mine (Gabon), was found in 1957 [30]. Francevillite occurs as cryptocrystalline veinlets and thin plates. Three other rare supergene uranyl vanadate minerals were found at the same locality in Gabon: vanuralite in 1963 [48], metavanuralite in 1970 [50], and curienite in 1968 [33]. It is of interest that the latter was first found as microcrystalline powder on crystals of francevillite. In 1965, strelkinite was discovered in the Jetisu Region (Kazakhstan) [46] as plates of nearly isometric form and sometimes powdery crusts along fractures in carbonaceous–siliceous Paleozoic shales.

Fine-grained yellow aggregates of margaritasite were found in 1980 in Peña Blanca uranium district (Mexico) in 1982 [37].

Four uranyl vanadate minerals were discovered in the XXIst century. Those are potassium uranyl sulfate–vanadate phase mathesiusite (described in 2013 at Svornost Mine, Jáchymov, Czech Republic [52]) and its ammonia-bearing analog ammoniomathesiusite (found in 2017 [53] on asphaltum/quartz matrix at Burro Mine, CO, USA).

Another potassium uranyl vanadate mineral, vandermeerscheite, occurs as yellow thin blade aggregates. It was found in 2017 in rather unusual district for secondary U-bearing minerals in Eifel Volcanic Fields (Germany) [47]. The mineral was named in honor of Eddy Van Der Meersche, a mineral collector from Ghent, Belgium.

The most recent natural uranyl vanadate reported up to date is the first U-bearing mineral that contains an essential portion of Sr, finchite [51]. Finchite is a member of the carnotite group and was found in Martin County (Texas, USA).

Most likely, the lack of structural diversity among the natural phases comes from close thermodynamic conditions of their formation.

3.2. Synthetic Uranyl Vanadates

The majority of known uranyl vanadates have a synthetic origin. The number of synthetic phases is nearly three times larger than the number of mineral phases, with a ratio of 57:17. In this chapter, we review synthesis pathways which were used to obtain the described compounds.

Synthetic uranyl vanadates can be divided into two groups: pure inorganic and mixed organic–inorganic compounds. The number of organic–inorganic compounds is smaller; it includes 20 compounds, while 37 can be attributed to purely inorganic compounds.

Fifteen known pure inorganic synthetic uranyl vanadates were synthesized using a hydrothermal technique. The temperature for the experiments ranged from 60° to 220° and the duration of experiments was from 12 h to 30 days. Uranyl nitrate hexahydrate, $(UO_2)(NO_3)_2{\cdot}6H_2O$, uranyl acetate hexahydrate, $UO_2(CH_3COO)_2{\cdot}6H_2O$, and $U_2V_2O_{11}$ were used as U-bearing component in most of the experiments. In a few syntheses, uranium oxide UO_3 (**40**, **53**) and $NaUV(H_2O)_4$ (**21**) were used as the source of uranium. Compound (**20**) was prepared using hydrothermal processing of **17**, and compound **18** was obtained via heating the single crystal of **19** in N_2 flow. The source of V in these experiments was usually V_2O_5, but in some cases, it was substituted by pure metal (**52**, **53**), V_2O_3 (**27**, **28**, **40**, **42**, **51**), or it was a component of uranium source (**21**, **24**, **25**, **26**, **29**).

Sixteen compounds among the synthetic uranyl vanadates were synthesized by solid-state reactions in a temperature range of 300–1200° and duration ranges from 2 h to 7 days. More often, uranium oxide, U_3O_8, was used as the U-bearing reagent, but in some of the experiments, $(UO_2)_3(VO_4)_2(H_2O)_5$ (**30**, **33**, **35**, **37**), $(UO_2)(NO_3)_2{\cdot}6H_2O$ (**49**, **50**), Na_2UO_4 (**32**) were used. In the case of compound **17**, $Na[(UO_2)(VO_4)]$ and UO_3 were used together. Vanadium oxide was used as the source of V^{5+} ion in most parts of syntheses, while for preparation of **17**, **30**, **33**, **34**, and **36,** the source of V was the same as for uranium.

Four uranyl vanadates (**32**, **38**, **44**, **45**) were synthesized by flux method. Uranyl nitrate hexahydrate $(UO_2)(NO_3)_2{\cdot}6H_2O$ and V_2O_5 were used as initial reagents, and calcium or strontium nitrates were used as a flux compound.

One uranyl vanadate was synthesized using the sealed quartz tube method (**39**). α-U_3O_8 was used as a uranium source, and the vanadium oxide was the source of V in this experiment. The temperature of the synthesis was 700°.

Eighteen mixed organic–inorganic uranyl vanadate compounds were obtained via the hydrothermal method in steel autoclaves with Teflon liners at a temperature of 180 °C and a duration range from 1 to 30 days. The reagents taken were uranyl nitrate and vanadium oxide dissolved in diluted acid. Only two compounds, **73** and **74,** were obtained via liquid–liquid diffusion technique. The duration of the experiments was from 7 days to several months. The reagents used were sodium metavanadate and uranyl nitrate. Crystals were grown at the boundary of an aqueous solution of vanadate salt and an ionic liquid solution of uranyl nitrate at room temperature. Such a specific reaction resulted in the formation of uranyl vanadate "nano-wheel" type clusters.

For the syntheses of organically templated uranyl vanadates, amine and diamine molecules of various shapes and sizes (lengths) of aliphatic counterparts were used.

3.3. Topological Analysis

Uranyl vanadate layered complexes and their topological depictions are represented in Figures 2–4. All currently known natural U–V compounds with insignificant presence of other oxyanions are based on layered complexes whose topologies are represented by only one type. The $5^14^13^1$ francevillite anion topology consists of edge-sharing dimers of pentagons, occupied by $(UO_2)_2{}^{4+}$, and edge-sharing dimers of squares, occupied by $(V_2O_8)^{6-}$ (Figure 2a,b). These infinite layers with composition $[(UO_2)_2(V_2O_8)]^{2-}{}_\infty$ underlie twelve of the fourteen known natural uranyl vanadate compounds. Among other synthetic phases with $5^14^13^1$ structural complex topologies, squares can be occupied by $(Cr^{5+}O_5)$, (NbO_5), or (TiO_5) groups. For minerals, however, only (VO_5) groups occur in this position. This topology is also widely represented among synthetic phases and is found in sixteen of them, including three mineral analogs.

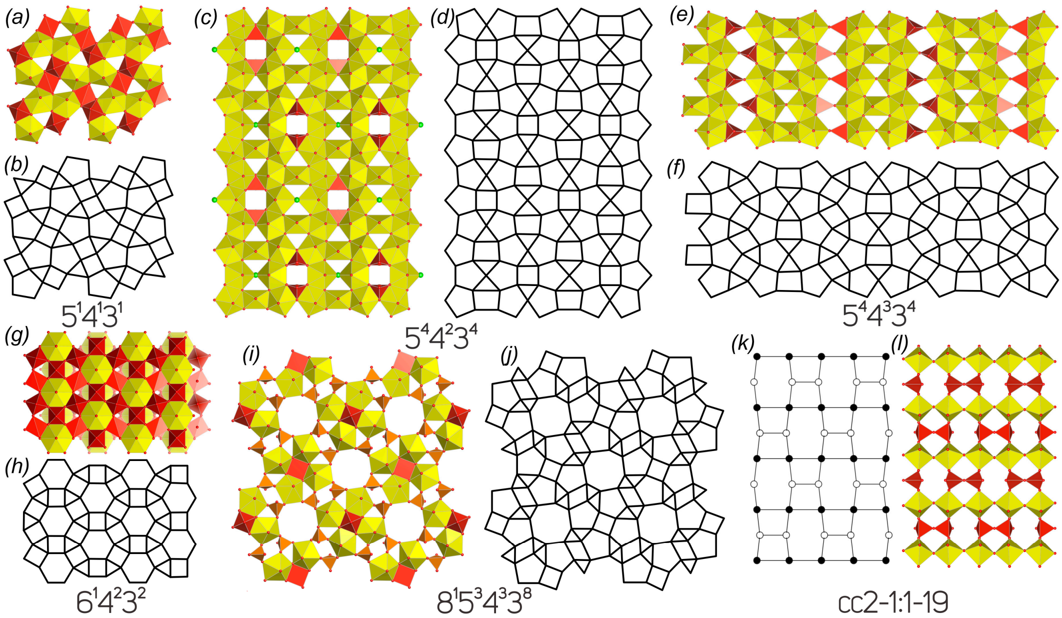

Figure 2. The 2D complexes in the crystal structures of natural and synthetic uranyl vanadates. Legend: U-bearing coordination polyhedra = yellow; V coordination polyhedra = orange; black nodes = U atoms, white nodes = V atoms.

The topology of $8^15^34^33^8$ (Figure 2i,j) type is unique for a mixed uranyl sulfate–vanadate mineral mathesiusite $K_5[(UO_2)_4(SO_4)_4(VO_5)](H_2O_4)]$ and its ammonium analog, ammoniomathesiusite $(NH_4)_{5.84}(UO_2)_4(SO_4)_4(VO_5)(H_2O)_4$. Heteropolyhedral sheets are formed by $[(UO_2)_4(SO_4)_4(VO_5)]^{5-}$ clusters, which are based on a cruciform composition of (VO_5) pyramids surrounded by four edge-shared uranyl pentagonal bipyramids.

The $5^44^23^4$ (β-U_3O_8) sheet topology (Figure 2c,d) involves infinite chains of edge-shared pentagons. Between the chains are squares half occupied by uranium atoms in distorted octahedral coordination and triangles half occupied by vacant $(VO_4)^{3-}$ tetrahedra.

The $5^44^33^4$ topology (Figure 2e,f) can be viewed as a sequential alternation of the β-U_3O_8 topology and the uranophane topology modules. The triangle positions in the uranophane module of this topology can be occupied by regular tetrahedra or irregular tetrahedra with a lone-electron pair. The orientation of the $(VO_4)^{3-}$ groups allows two geometric isomers to be distinguished (Figure 3).

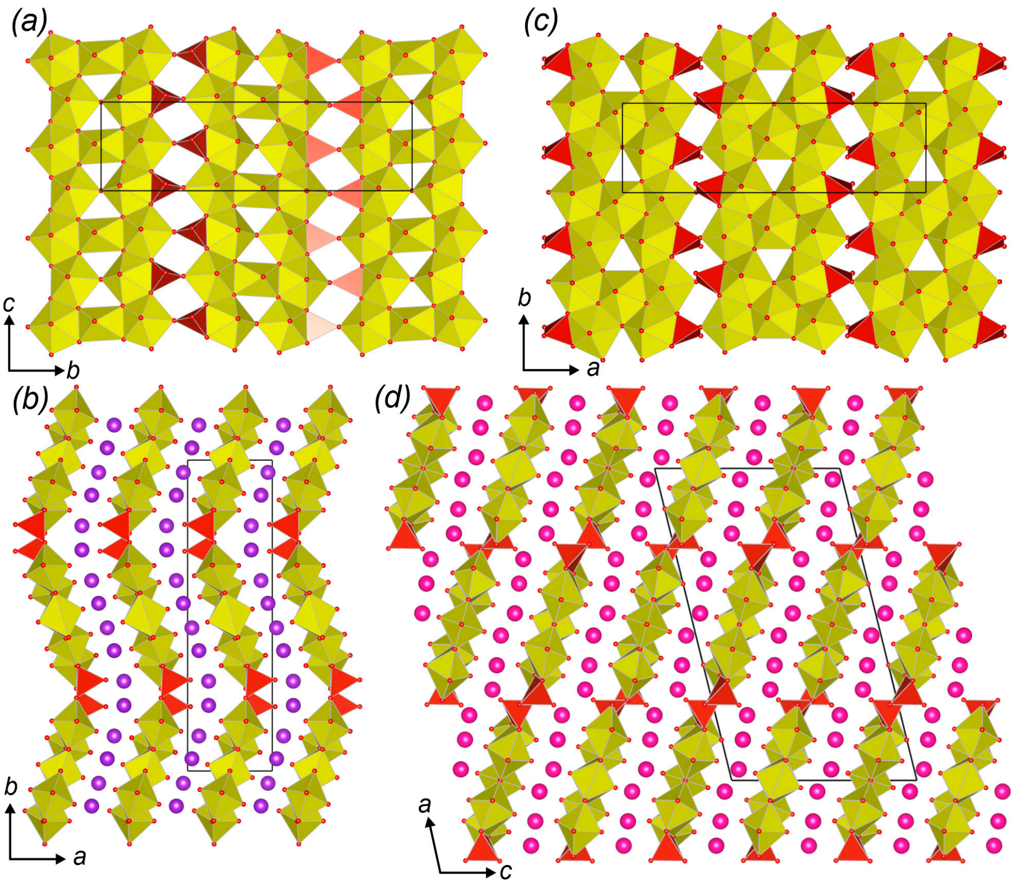

Figure 3. Uranyl vanadate layers and the crystal structure projections along the layers of **32**–**34** (**a**,**b**), **35** (**c**,**d**). Legend: see Figure 1; Na = purple, Rb = pink.

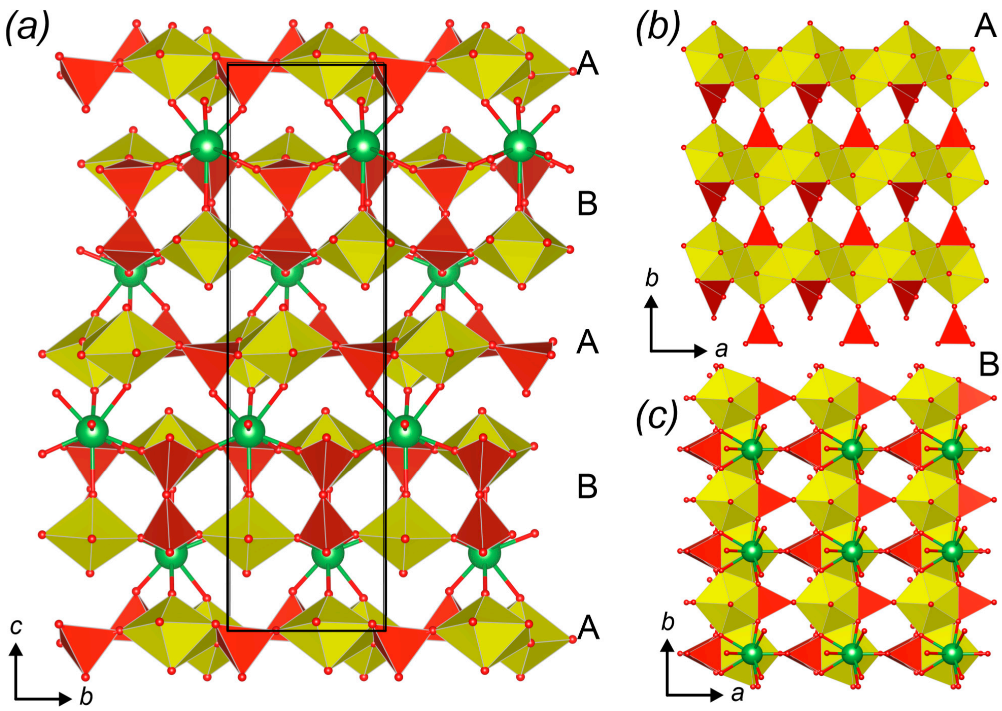

Figure 4. Uranyl vanadate layers and the crystal structure projections along the layers of **39**. Legend: see Figure 1.

The $6^1 4^2 3^2$ sheet-anion topology (Figure 2g,h) consists of $6^1 4^6 3^6$ clusters. Each hexagonal position is occupied by the uranyl group and surrounded by six squares occupied by (VO_5) pyramids. The layers are pairwise connected by van der Waals bonding, forming the structure with the participation of additional Cs^+ interstitial cations between pairs.

One of the few uranyl vanadate compounds in which the layered structural complex is formed by vertex-shared polyhedra is **37** (Figure 2k,l). The complex is formed by infinite chains of tetragonal bipyramids $[UO_6]^{6-}$, which are connected by vertex-shared divanadate groups V_2O_7.

The structure of **39**, $La(UO_2)_2(VO_4)(V_2O_7)$ (Figure 4) is based upon layers derived from uranophane-type topology. Uranyl ions occupy pentagonal sites, while vanadate ions occupy triangular sites, forming $[(UO_2)(VO_4)]^-$ sheets. Lanthanum ions partially replace the uranyl ions, forming a new sheet of $[La(UO_2)(VO_4)_2]^-$ composition. These sheets are linked via divanadate ions, creating $[La(UO_2)(V_2O_7)]^+$ double layers. The overall three-dimensional structure alternates between these double layers and single uranophane-type sheets stabilized by the substitution of trivalent REE cations such as La.

The frameworks of compounds **47–50** can be described as various combinations of one-dimensional $_\infty[UO_5]^{4-}$ uranyl chains and layers of the types I—$_\infty[(UO_2)_2(VO_4)_3]^{5-}$ (Figure 5a) and II—$_\infty[(UO_2)(VO_4)_2]^{4-}$ (Figure 5b) [74]. The framework corresponding to compound **48** is represented by the I–I configuration (Figure 5c), compound **47** corresponds to the II–II configuration (Figure 5e), while compounds **49** and **50** exhibit an alternating layer arrangement of the I–II types (Figure 5d).

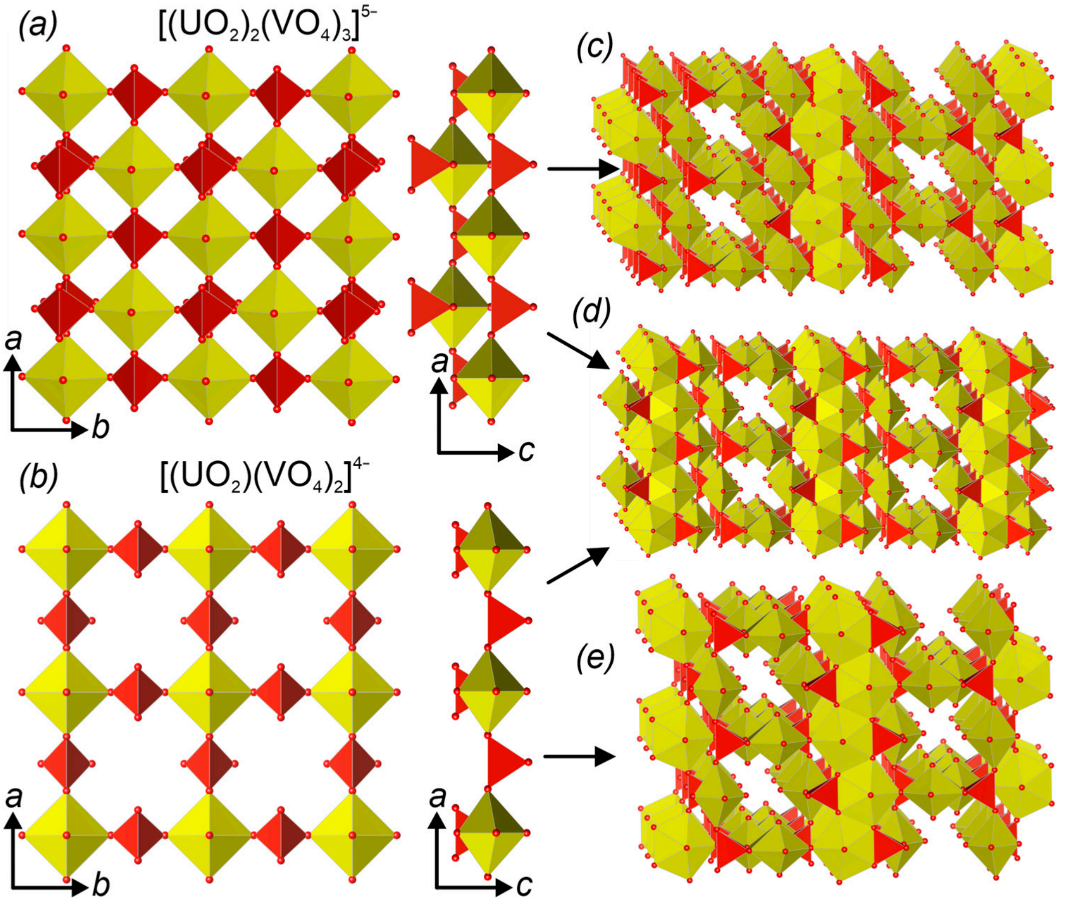

Figure 5. Various combinations of layered complexes (**a**,**b**) and infinite $[UO_5]^{4-}{}_\infty$ chains in the frameworks of compounds **48** (**c**), **49–50** (**d**), **47** (**e**).

The frameworks of compounds **47–50** were also analyzed in terms of primitive proper tilings. Calculations revealed that the 3D cation net of compound **47** consists of two types of tiles [$5^2.8^2$] (Figure 6d) and [$3^4.8^2$] (Figure 5e). To describe the cationic nets of compounds **43–45**, this set of tiles must be supplemented with an additional tile [58] (Figure 6f). The inclusion of the [58] tile in compounds **48–50** reflects an increase in structural complexity. The tiling pattern of the network in the structure of compound **48** differs from those of compounds **49** and **50** in the ratio of the tile types.

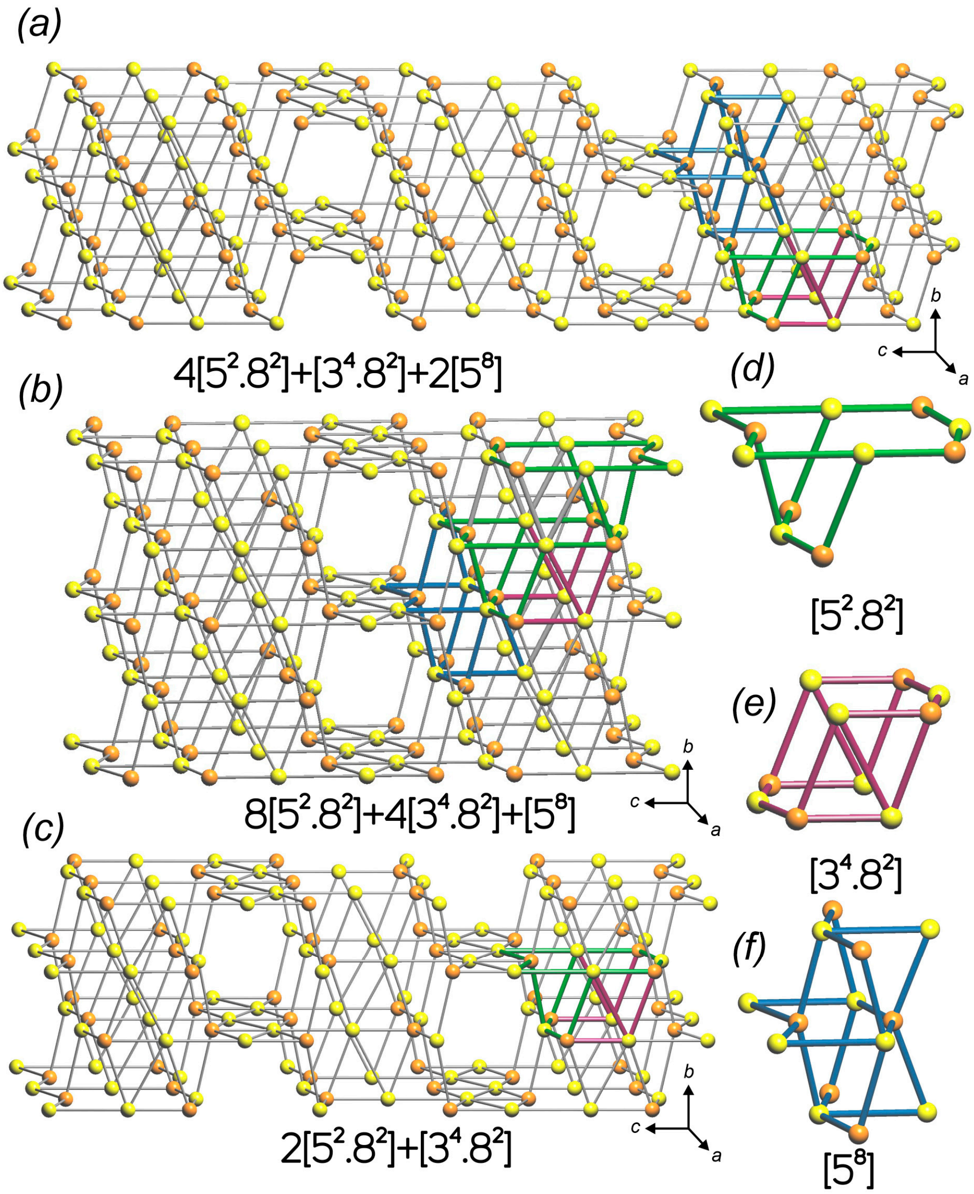

Figure 6. The 3D net representation and natural tilings in the structures of **48** (**a**), **49–50** (**b**), **47** (**c**). Corresponding tiles (**d**–**f**). Legend: U = yellow, V = orange.

The frameworks of **46**, $Pb(UO_2)(V_2O_7)$ (Figure 7a,b) and **47**, $Sr(UO_2)(V_2O_7)$ (Figure 7c) are closely related and are defined by natural tiles [$6^2.8^2$] (Figure 7e), a polyhedron composed of hexagonal and octagonal faces [$8^2.10^2$] (Figure 7d), larger tile featuring octagonal and decagonal faces. These frameworks exhibit topological polymorphism, where slight variations in ionic radii result in distinct structural differences [67]. The approximate ranges for ionic radii are $Ca^{2+} \approx$ 1.12–1.18 Å, $Pb^{2+} \approx$ 1.23–1.29 Å. These slight differences in ionic radii can affect the way these ions fit into the crystal lattice and interact with the surrounding UO_2 and V_2O_7. Sr^{2+}, being slightly larger on average, may lead to more open or expanded structures, while Pb^{2+}, being marginally smaller, could result in denser arrangements.

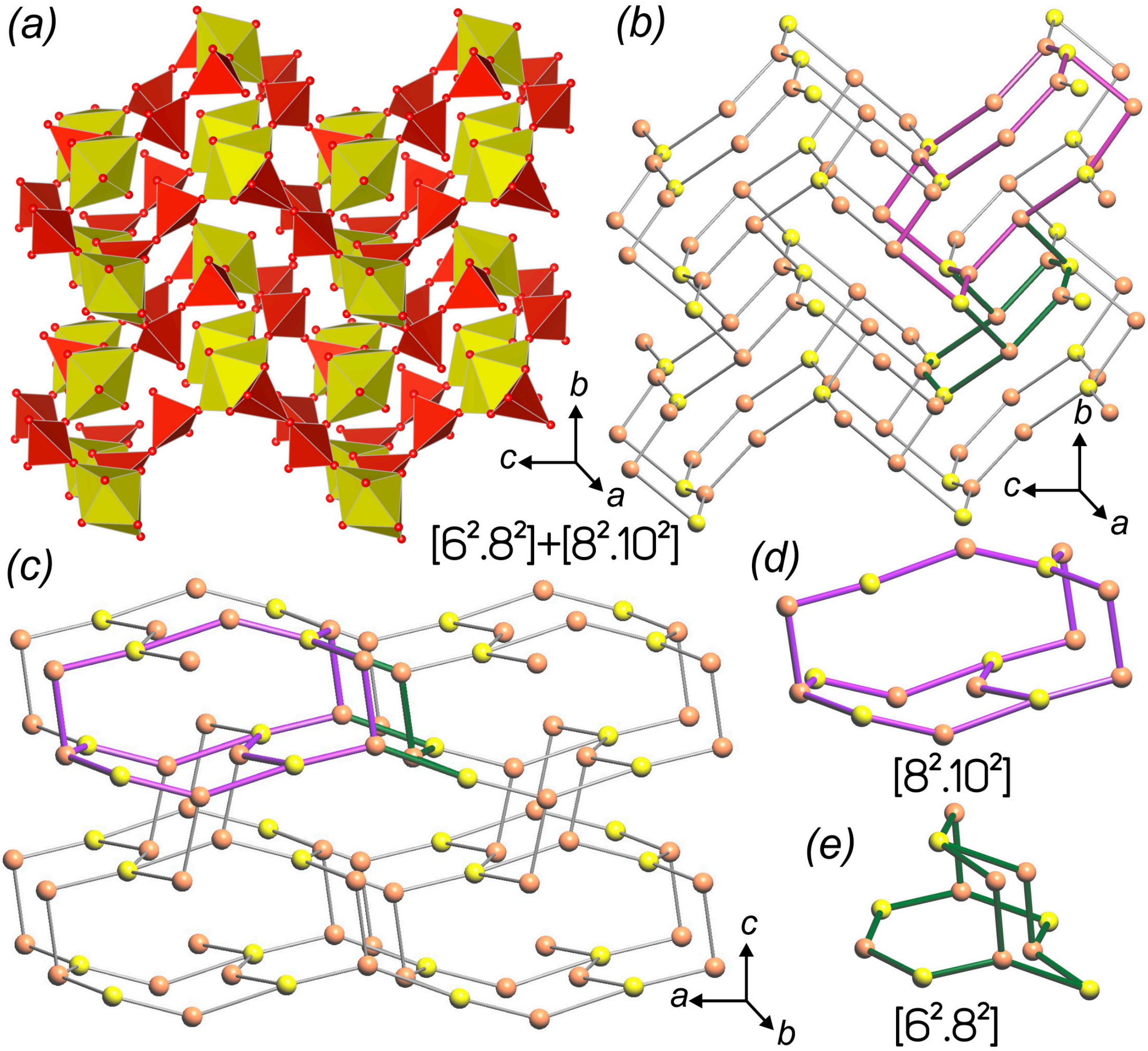

Figure 7. Framework architecture in the crystal structure of **46** (**a**). A 3D net representation and natural tilings in the structures of **46** (**b**) and **45** (**c**). Corresponding tiles (**d**,**e**). Legend: see Figure 6.

3.4. Crystal Structures vs. Synthesis Conditions

The structural complexity of layered uranyl vanadates is a multifaceted topic influenced by various cations, organic molecules, and inherent U–V units. Inorganic cations in the interstitial spaces (including lanthanides) perform a dual function: they promote charge balance and influence the structural integrity of the layered compounds. Organic molecules can play a similar role, also occupying interlayer spaces and influencing the spacing and symmetry of the U–V layers and frameworks.

The francevillite topology is the most prevalent structural arrangement observed among uranyl vanadates. Compounds within this classification can be systematically categorized based on their minimum interlayer spacing and the complexity of their crystalline structures (Figure 8).

Compounds that incorporate inorganic interlayer cations, excluding lanthanides, exhibit the smallest interlayer spacing. The smaller ionic radii of these cations allow for tighter packing of the layers, reducing the overall cell volume. This compact arrangement limits structural variability, resulting in relatively low complexity. In contrast, compounds with organic interlayer cations exhibit moderately larger cell volumes due to the bulkier nature of organic molecules, which increases the spacing between layers. These organic species also introduce more degrees of freedom in layer stacking, bonding interactions, and the presence of geometrical isomers of the structural unit, leading to increased structural complexity.

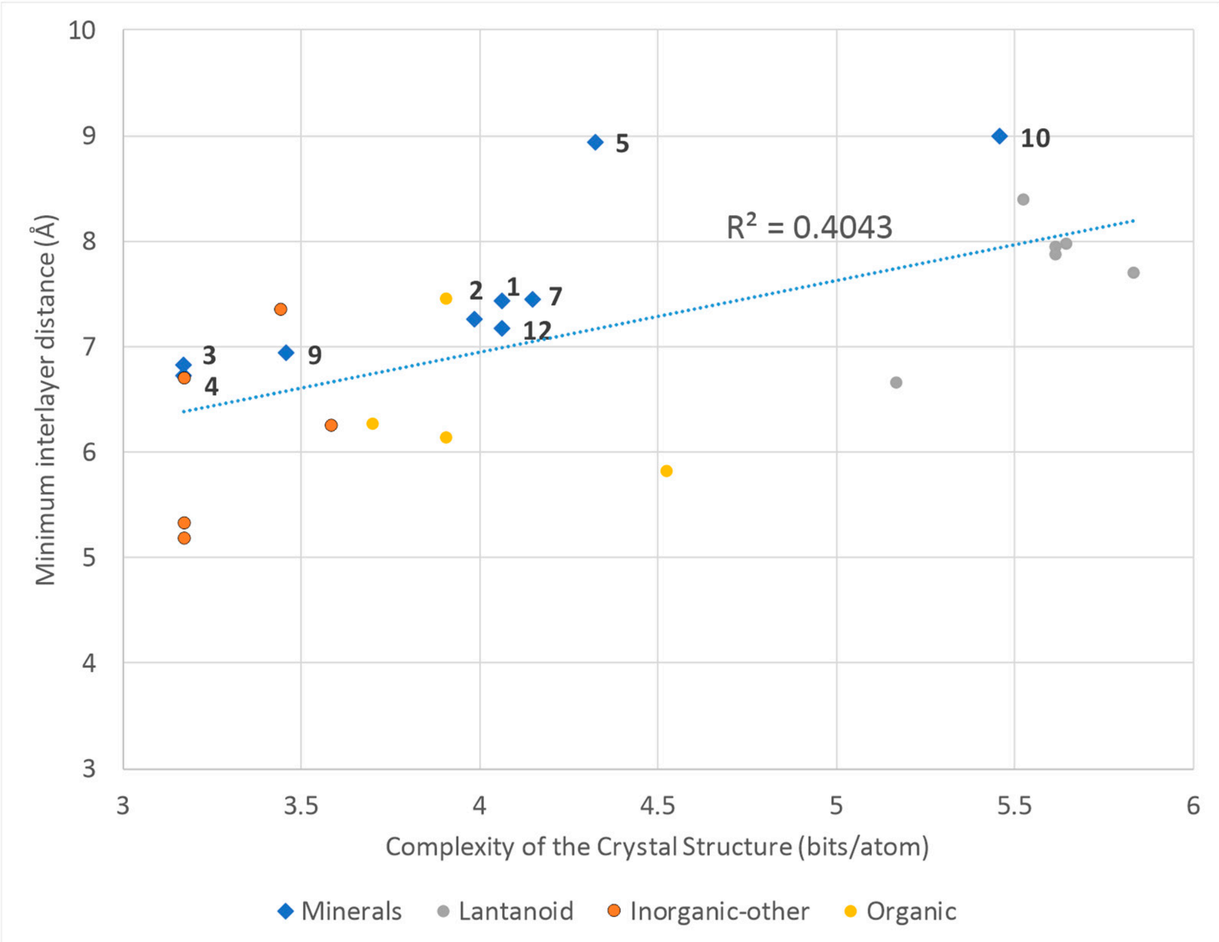

Figure 8. Relationship between minimum interlayer distance (in Å) and crystal structure complexity (in bits/atom) for compounds based on the francevillite topology. The dotted blue line is the trend line. R^2—coefficient of determination.

The highest levels of complexity, interlayer distances, and largest cell volumes are associated with compounds that contain lanthanide ions (Figure 9). Several factors may account for the diversity of geometrical isomers found in carnotite-type layers. Notably, the larger ionic radius of La^{3+} and its unique electronic configuration play significant roles in this context.

The degree of hydration also plays a crucial role in determining structural complexity. For example, vanuralite mineral is notable for having a high content of molecular H_2O within its structure. This incorporation of H_2O molecules not only influences interlayer spacing but also affects H-bonding interactions, which can stabilize or destabilize specific structural motifs.

Uranophane topology represents a distinctive structural arrangement that, although not observed in natural uranyl vanadates, is frequently encountered in synthetic compounds. A defining feature of these layers is the varied orientation of the vanadium tetrahedra, which leads to the formation of a multitude of geometric isomers (Figure 10). The rotational orientation and spatial arrangement of these tetrahedra are influenced by interlayer polyhedra of uranium and other cations, resulting in a rich diversity of structural configurations.

Compound **37** exhibits a porous three-dimensional framework constructed from layers that display uranophane topology. In this structure, the layers consist of UO_7 pentagonal bipyramids interconnected with distorted monomeric VO_4 tetrahedra. The connectivity among these components is facilitated by additional UO_7 pillars (Figure 10g).

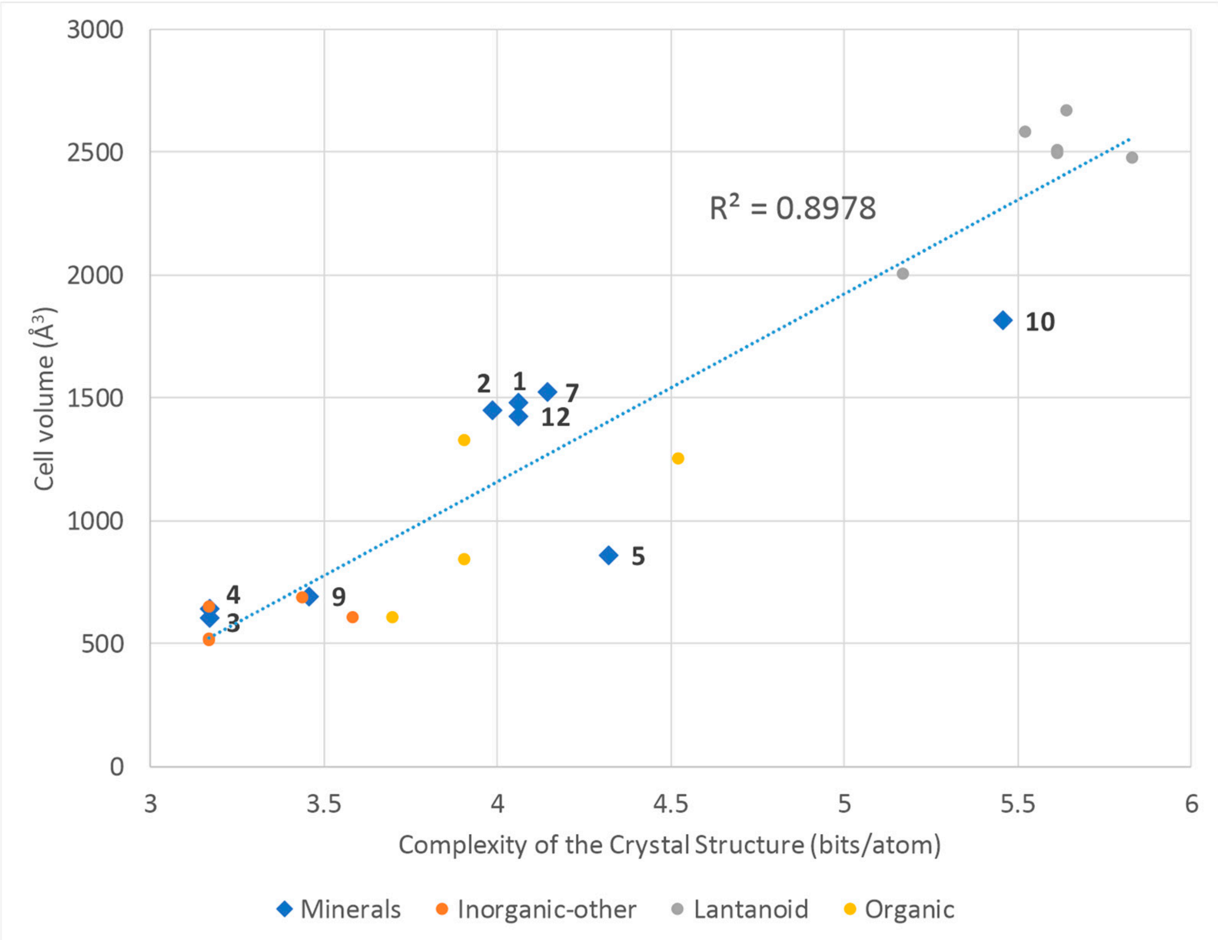

Figure 9. Relationship between cell volume (in $Å^3$) and crystal structure complexity (in bits/atom) for compounds based on the francevillite topology. The dotted blue line is the trend line. R^2—coefficient of determination.

The introduction of europium ions (Eu^{3+}) in compound **51** indeed leads to a significant reduction in the overall symmetry of the structure, as well as within the uranophane-type layers due to the orientation of the VO_4 tetrahedra (Figure 10h).

Comparing structural particularities with the syntheses conditions, some observations can be described. Thus, 9 out of 20 compounds with structures based on U–V layers were obtained as a result of high-temperature solid-state syntheses. Compound **18**, obtained under high-temperature conditions, has the same symmetry as compound **29**, based on the same layer topology, but was obtained through medium-temperature hydrothermal synthesis.

Framework structures bring another tendency. The crystal structure of **46**, which was synthesized in the course of the solid-state reaction, has a lower symmetry than that of **45**, obtained by the flux method and higher temperature. Also, there is a tendency toward the formation of larger tiles among lower–medium temperature compounds (**51–54** vs. **45–48**).

The crystal structures of compounds **41** and **42** are based on frameworks constructed by tiles of the $[8^3] + [3^4.8^2] + [3^4.4^4.8.10^2]$ topological type. These compounds have close symmetry and were synthesized by heating with temperatures ranging from 60 to 200 °C, which demonstrates the stability of the current architecture.

Among the variety of synthetic uranyl vanadates, a group of compounds stands out, whose structures are built from frameworks based on layered complexes with uranophane topological type. This group includes compounds with inorganic cations, compounds with protonated molecules of various amines, and compounds without additional cations. As has been shown in recent papers [78–80], such frameworks based on uranophane layers turned out to be very resistant to the inclusion of organic molecules of various shapes and sizes into the pore space. Moreover, depending on the molecule used, the framework changes its geometry, adapting to the stereochemistry of a particular molecule. Thus, organic molecules in the studied systems act as pillars—a common process in clay science [85,86].

Figure 11 shows a trend toward increasing structural complexity parameters depending on the distance between the uranophane layers in a framework: the greater the distance, the higher the complexity values. A similar tendency was recently shown for the family of organically templated layered uranyl sulfates and selenates [87]. The mechanism of a certain topology of U-bearing layer control by organic molecules has also been described earlier [88,89]. Thus, large non-planar molecules like cyclohexylamine and tert-butylamine result in the largest interlayer distances (green dots in Figure 11); smaller branchy molecules like tetramethylammonium are arranged slightly lower (dark-blue dots in Figure 11); significantly smaller interlayer distance is observed for chain diamine molecules (light-blue dots in Figure 11), which is explained by their arrangement parallel to the layers. The top right corner of the graph corresponds to the Eu-bearing framework structure. It means that complex and large $[EuO_2(H_2O)_{5\text{-}6}]$ polyhedra are comparable to and can act as large and branchy organic cations. The lower left point on a graph corresponds to the pure uranyl vanadate framework without any additional molecules and ions, in which all organically templated framework structures with francevillite and uranophane type of layers transform with heating [78].

For uranyl vanadates based on the uranophane topology, no clear dependence of structural complexity on unit cell volume has been identified (Figure 12). This may be attributed to the structural and symmetry diversity within this group. In contrast, among the compounds with the francevillite type of topology, all crystal structures were based on layered complexes, and most belong to the monoclinic crystal system. For a more detailed investigation of the relationship between crystal structure complexity and unit cell volume, additional computational parameters can be utilized [90].

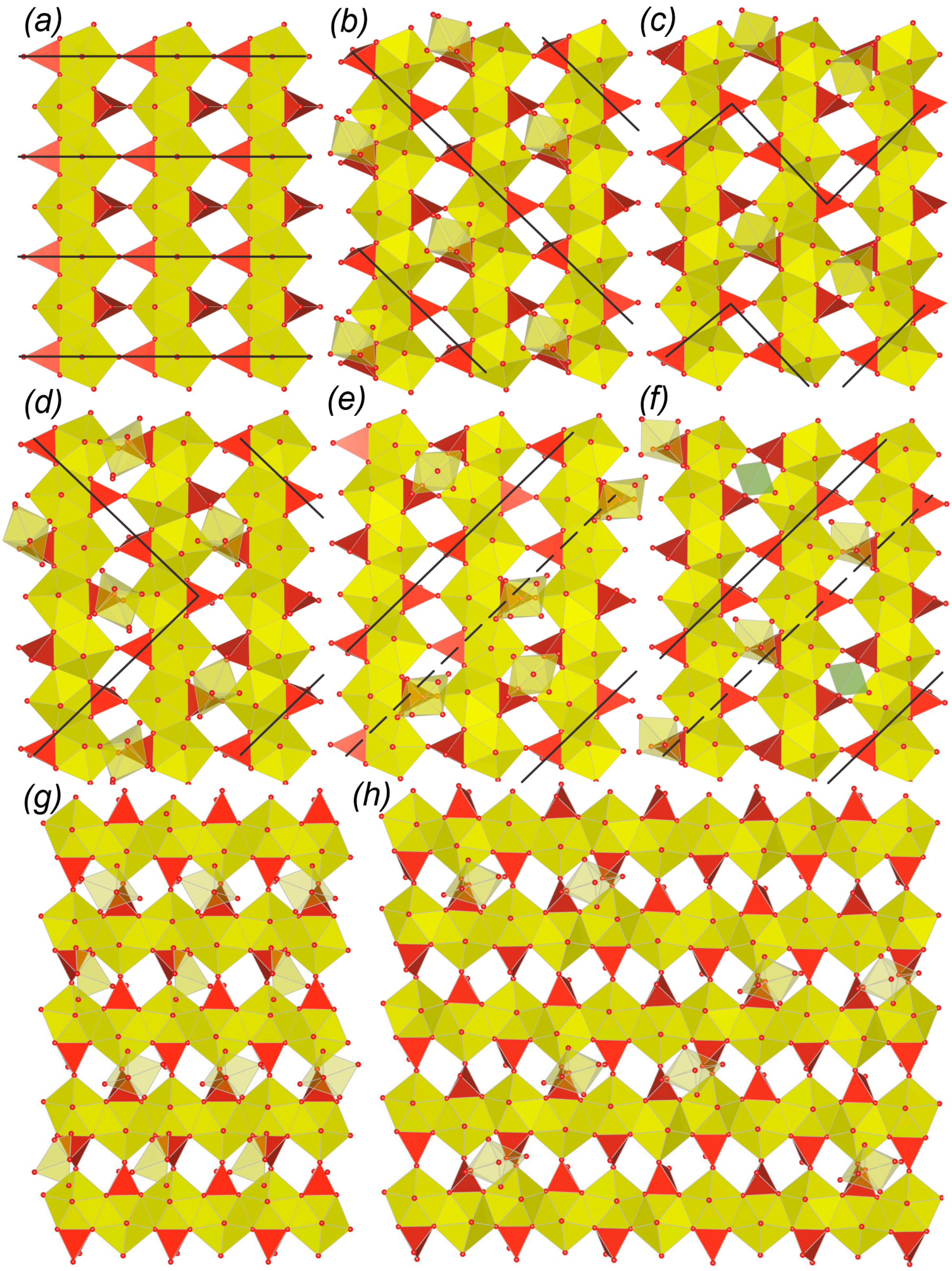

Figure 10. The uranophane-type sheet in **60** (**a**); (**b**) pillared uranophane sheets-I in **61**; (**c**) pillared uranophane sheets-II in **62–67**; (**d**) pillared uranophane sheets-IV in **70–72** pillared uranophane sheets-III in **68** (**e**) and **69** (**f**); framework based on the uranophane sheets in **42** (**g**) and **51** (**h**) Solid lines denote polyhedra with vertices pointing downwards. Dashed lines denote polyhedra with alternating orientations.

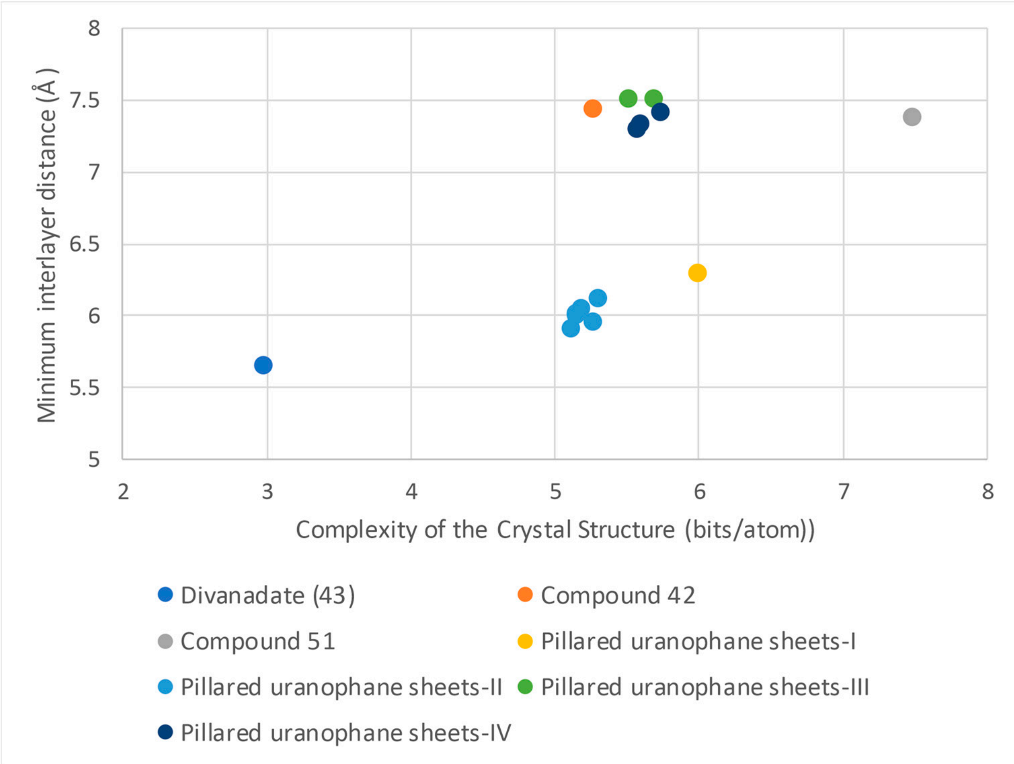

Figure 11. Relationship between minimum interlayer distance (in Å) crystal structure complexity (in bits/atom) for compounds based on the uranophane topology.

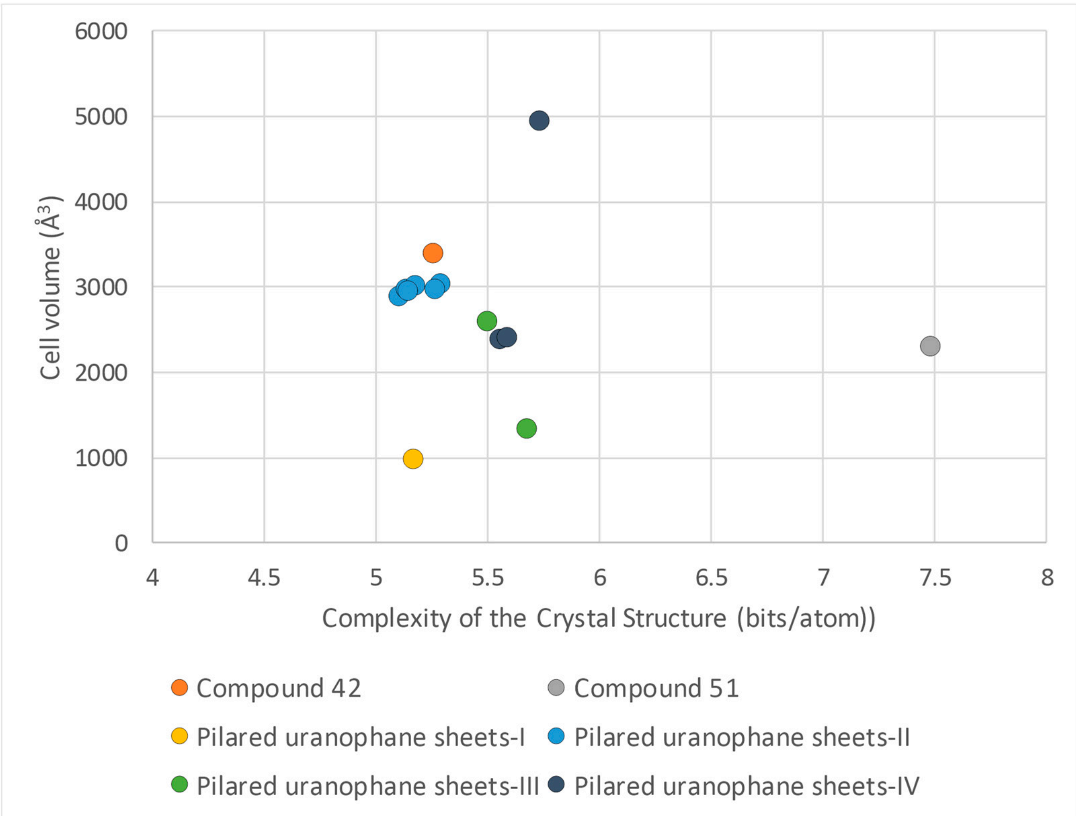

Figure 12. Relationship between cell volume (in Å^3) and crystal structure complexity (in bits/atom) for compounds based on the uranophane topology.

4. Conclusions

Analysis of synthetic compound preparation protocols illustrates that the dominant methods of obtaining inorganic synthetic uranyl vanadates are hydrothermal and solid-state techniques. The temperature chosen for hydrothermal syntheses is not higher than 220 °C, while solid-state reactions are subjected to a much higher temperature range of approximately 700–1200 °C. Only a few compounds were synthesized via different techniques like flux, sealed quartz tube methods, or such techniques as heating in a steam of dry nitrogen. All, except for two mixed organic–inorganic compounds, were prepared using a hydrothermal technique at 180 °C. It is of interest that the majority of synthetic compounds, both pure inorganic or organically templated, have their structures based upon mineral-like substructural units of francevillite, uranophane, U_3O_8, and other common topological types, and not even one compound among 57 studied was obtained from simple aqueous solutions at room temperature. This allows us to assume that even under natural conditions, elevated temperatures are required for the formation of isotypic uranyl vanadate minerals, especially in the case of industrially developed thick strata.

The structural complexity parameters for natural uranyl vanadates directly depend on the unit cell volume. Keeping in mind that all minerals possess layered structural architecture, it means that structural complexity increases with the increase in the interlayer spacing, which, in turn, depends on the size of cations or water–cationic complexes arranged in the interlayer space. This tendency similarly works for organic molecules, which are incorporated into the uranyl vanadate frameworks. It can also be concluded that the architecture of the uranyl vanadate substructural units defines the complexity of the entire crystal structure.

Author Contributions: All authors contributed equally to the conceptualization, methodology, investigation, writing—original draft preparation, writing—review and editing, and visualization. All authors have read and agreed to the published version of the manuscript.

Funding: This work was supported by the Russian Science Foundation (grant No. 23-17-00080).

Data Availability Statement: Not applicable.

Acknowledgments: We want to thank anonymous reviewers for their constructive comments on this manuscript. Access to structural databases was provided by the X-ray Diffraction Centre of St. Petersburg State University.

Conflicts of Interest: The authors declare no conflicts of interest.

References

1. Scott, W.W. Determination of Uranium in Carnotite Ore. *Ind. Eng. Chem. Anal. Ed.* **1932**, *4*, 244. [CrossRef]
2. Bruyn, K. *Uranium Country*; University of Colorado Press: Boulder, CO, USA, 1955.
3. Robison, R. Colorado Uranium. In *Mining and Selling Radium and Uranium*; Springer: Cham, Switzerland, 2015; pp. 109–131. [CrossRef]
4. Sidorenko, G.A. *Crystal Chemistry of Uranium Minerals*; Atomizdat: Moscow, Russia, 1978; 220p.
5. Krivovichev, S.V.; Burns, P.C. Actinide compounds containing hexavalent cations of the VI group elements (S, Se, Mo, Cr, W). In *Structural Chemistry of Inorganic Actinide Compounds*; Krivovichev, S.V., Burns, P.C., Tananaev, I.G., Eds.; Elsevier: Amsterdam, The Netherlands, 2007; pp. 95–182.
6. Krivovichev, S.V.; Plášil, J. Mineralogy and Crystallography of Uranium. In *Uranium: From Cradle to Grave*; Burns, P.C., Sigmon, G.E., Eds.; MAC Short Courses; Association of Canada: Winnipeg, MB, Canada, 2013; Volume 43, pp. 15–119.
7. Gurzhiy, V.V.; Kuporev, I.V.; Kovrugin, V.M.; Murashko, M.N.; Kasatkin, A.V.; Plášil, J. Crystal Chemistry and Structural Complexity of Natural and Synthetic Uranyl Selenites. *Crystals* **2019**, *9*, 639. [CrossRef]
8. Gurzhiy, V.V.; Kalashnikova, S.A.; Kuporev, I.V.; Plášil, J. Crystal Chemistry and Structural Complexity of the Uranyl Carbonate Minerals and Synthetic Compounds. *Crystals* **2021**, *11*, 704. [CrossRef]

9. Kuporev, I.V.; Kalashnikova, S.A.; Gurzhiy, V.V. Crystal Chemistry and Structural Complexity of the Uranyl Molybdate Minerals and Synthetic Compounds. *Crystals* **2024**, *14*, 15. [CrossRef]
10. Lafuente, B.; Downs, R.T.; Yang, H.; Stone, N. The power of databases: The RRUFF project. In *Highlights in Mineralogical Crystallography*; Armbruster, T., Danisi, R.M., Eds.; De Gruyter: Berlin, Germany, 2015; pp. 1–30.
11. Burns, P.C.; Miller, M.L.; Ewing, R.C. U^{6+} minerals and inorganic phases: A comparison and hierarchy of structures. *Can. Mineral.* **1996**, *34*, 845–880.
12. Lussier, A.J.; Lopez, R.A.K.; Burns, P.C. A revised and expanded structure hierarchy of natural and synthetic hexavalent uranium compounds. *Can. Mineral.* **2016**, *54*, 177–283. [CrossRef]
13. Hawthorne, F.C. Graphical enumeration of polyhedral clusters. *Acta Crystallogr. A* **1983**, *39*, 724–736. [CrossRef]
14. Krivovichev, S.V. Topological complexity of crystal structures: Quantitative approach. *Acta Crystallogr. A* **2012**, *68*, 393–398. [CrossRef]
15. Krivovichev, S.V. Structural complexity of minerals: Information storage and processing in the mineral world. *Mineral. Mag.* **2013**, *77*, 275–326. [CrossRef]
16. Krivovichev, S.V. Which inorganic structures are the most complex? *Angew. Chem. Int. Ed.* **2014**, *53*, 654–661. [CrossRef]
17. Blatov, V.A.; Delgado-Friedrichs, O.; O'Keeffe, M.; Proserpio, D.M. Three-periodic nets and tilings: Natural tilings for nets. *Acta Cryst.* **2007**, *A63*, 418–425. [CrossRef]
18. Aksenov, S.M.; Mackley, S.A.; Deyneko, D.V.; Taroev, V.K.; Tauson, V.L.; Rastsvetaeva, R.K.; Burns, P.C. Crystal chemistry of compounds with lanthanide based microporous heteropolyhedral frameworks: Synthesis, crystal structures, and luminescence properties of novel potassium cerium and erbium silicates. *Micropor. Mesopor. Mater.* **2019**, *284*, 25–35. [CrossRef]
19. Chukanov, N.V.; Aksenov, S.M.; Rastsvetaeva, R.K. Structural chemistry, IR spectroscopy, properties, and genesis of natural and synthetic microporous cancrinite- and sodalite-related materials: A review. *Micropor. Mesopor. Mater.* **2021**, *323*, 111098. [CrossRef]
20. Blatov, V.A.; Shevchenko, A.P.; Proserpio, D.M. Applied topological analysis of crystal structures with the program package ToposPro. *Cryst. Growth. Des.* **2014**, *14*, 3576–3586. [CrossRef]
21. Krivovichev, S.V. Structural complexity of minerals and mineral parageneses: Information and its evolution in the mineral world. In *Highlights in Mineralogical Crystallography*; Danisi, R., Armbruster, T., Eds.; Walter de Gruyter: Berlin, Germany, 2015; pp. 31–73.
22. Krivovichev, S.V. Structural complexity and configurational entropy of crystalline solids. *Acta Crystallogr. B* **2016**, *72*, 274–276. [CrossRef] [PubMed]
23. Gurzhiy, V.V.; Tyumentseva, O.S.; Izatulina, A.R.; Krivovichev, S.V.; Tananaev, I.G. Chemically Induced Polytypic Phase Transitions in the $Mg[(UO_2)(TO_4)_2(H_2O)](H_2O)_4$ (*T* = S, Se) System. *Inorg. Chem.* **2019**, *58*, 14760–14768. [CrossRef] [PubMed]
24. Gurzhiy, V.V.; Tyumentseva, O.S.; Belova, E.V.; Krivovichev, S.V. Chemically induced symmetry breaking in the crystal structure of guanidinium uranyl sulfate. *Mendeleev Commun.* **2019**, *29*, 408–410. [CrossRef]
25. Tyumentseva, O.S.; Kornyakov, I.V.; Britvin, S.N.; Zolotarev, A.A.; Gurzhiy, V.V. Crystallographic Insights into Uranyl Sulfate Minerals Formation: Synthesis and Crystal Structures of Three Novel Cesium Uranyl Sulfates. *Crystals* **2019**, *9*, 660. [CrossRef]
26. Kornyakov, I.V.; Kalashnikova, S.A.; Gurzhiy, V.V.; Britvin, S.N.; Belova, E.V.; Krivovichev, S.V. Synthesis, characterization and morphotropic transitions in a family of $M[(UO_2)(CH_3COO)_3](H_2O)_n$ (*M* = Na, K, Rb, Cs; n = 0–1.0) compounds. *Z. Kristallogr.* **2020**, *235*, 95–103. [CrossRef]
27. Kornyakov, I.V.; Tyumentseva, O.S.; Krivovichev, S.V.; Gurzhiy, V.V. Dimensional evolution in hydrated K+-bearing uranyl sulfates: From 2D-sheets to 3D frameworks. *Cryst. Eng. Comm.* **2020**, *22*, 4621–4629. [CrossRef]
28. Gurzhiy, V.V.; Plasil, J. Structural complexity of natural uranyl sulfates. *Acta Crystallogr. B* **2019**, *75*, 39–48. [CrossRef] [PubMed]
29. Krivovichev, V.G.; Krivovichev, S.V.; Charykova, M.V. Selenium Minerals: Structural and Chemical Diversity and Complexity. *Minerals* **2019**, *9*, 455. [CrossRef]
30. Branche, G.; Ropert, M.E.; Chantret, F.; Morignat, B.; Pouget, R. La francevillite, nouveau minéral uranifère. *C. R. Hebd. Séances Acad. Sci.* **1957**, *245*, 89–91.
31. Mereiter, K. Crystal structure refinement of two francevillites, $(Ba,Pb)[(UO_2)_2V_2O_8]\cdot 5H_2O$. *Neues Jahrb. Für Mineral. Monatshefte* **1986**, *1986*, 552–560.
32. Frost, R.L.; Čejka, J.; Weier, M.L.; Martens, W.; Henry, D.A. Vibrational spectroscopy of selected natural uranyl vanadates. *Vib. Spectrosc.* **2005**, *39*, 131–138. [CrossRef]
33. Cesbron, F.; Morin, N. Une nouvelle espèce minérale: La curiénite. Étude de la série francevillite-curiénite. *Bull. Soc. Fr. Mineral. Cristallogr.* **1968**, *91*, 453–459. [CrossRef]
34. Borène, J.; Cesbron, F. Structure cristalline de la curiénite $Pb(UO_2)_2(VO_4)_2\cdot 5H_2O$. *Bull. Soc. Fr. Mineral. Cristallogr.* **1971**, *94*, 8–14. [CrossRef]
35. Friedel, C.; Cumenge, E. Sur un nouveau minerai d'urane. *Bull. Soc. Fr. Mineral. Cristallogr.* **1899**, *22*, 26–29.
36. Appleman, D.E.; Evans, H.T. The crystal structure of carnotite. *Acta Crystallogr.* **1957**, *10*, 765.
37. Wenrich, K.J.; Modreski, P.J.; Zielinski, R.A.; Seeley, J.L. Margaritasite: A new mineral of hydrothermal origin for the Peña Blanca uranium district, Mexico. *Am. Mineral.* **1982**, *67*, 1273–1289.

38. Faudoa-Gómez, F.G.; Fuentes-Cobas, L.E.; Esparza-Ponce, H.E.; Canche-Tello, J.G.; Reyes-Cortés, I.A.; Fuentes-Montero, M.E.; Eichert, D.M.; Rodríguez-Guerra, Y.; Montero-Cabrera, M.-E. Geological and Crystallochemical Characterization of the Margaritasite–Carnotite Mineral from the Uranium Region of Peña Blanca, Chihuahua, Mexico. *Minerals* **2024**, *14*, 431. [CrossRef]
39. Vaes, J.F.; Kerr, P.F. Sengierite: A preliminary description. *Am. Mineral.* **1949**, *34*, 109–120.
40. Hutton, C.O. Sengierite from Bisbee, Arizona. *Am. Mineral.* **1957**, *42*, 408–411.
41. Piret, P.; Declercq, J.P.; Wauters-Stoop, D. Structure cristalline de la sengiérite. *Bull. Mineral.* **1980**, *103*, 176–178.
42. Nenadkevich, K.A. Tyuyamunite—A new mineral. *Bull. Acad. Imp. Sci.* **1912**, *6*, 945–946.
43. Weeks, A.D.; Thompson, M.E. Identification and occurrence of uranium and vanadium minerals from the Colorado Plateaus: Tyutamunite and metatyuyamunite. *Bull. United States Geol. Surv.* **1954**, *1009-B*, 37–38.
44. Stern, T.W.; Stieff, L.R.; Girhard, M.N.; Meyrowitz, R. The occurrence and properties of metatyuyamunite, $Ca(UO_2)_2(VO_4)_2{\cdot}3$-$5H_2O$. *Am. Mineral.* **1956**, *41*, 187–201.
45. Burciaga-Valencia, D.C.; Reyes-Cortes, M.; Reyes-Rojas, A.; Renteria-Villalobos, M.; Esparza-Ponce, H.; Fuentes-Cobas, L.; Fuentes-Montero, L.; Silva-Saenz, M.; Herrera-Peraza, E.; Munoz, A.; et al. Characterization of uranium minerals from Chihuahua using synchrotron radiation. *Rev. Mex. Física* **2010**, *56*, 75–81.
46. Alekseeva, M.A.; Chernikov, A.A.; Shashkin, D.P.; Kon'kova, E.A.; Gavrilova, I.N. Strelkinite, a new uranyl vanadate. *Zap. Vsesoyuznogo Mineral. Obs.* **1974**, *103*, 576–580. [CrossRef]
47. Plášil, J.; Kampf, A.R.; Škoda, R.; Čejka, J. Vandermeerscheite, a new uranyl vanadate related to carnotite from Eifel, Germany. *J. Geosci.* **2019**, *64*, 219–227. [CrossRef]
48. Branche, G.; Bariand, P.; Chantret, F.; Pouget, R.; Rimsky, A. La vanuralite, nouveau minéral uranifère. *C. R. Hebd. Séances Acad. Sci.* **1963**, *256*, 5374–5376.
49. Plášil, J. Crystal structure of vanuralite, $Al[(UO_2)_2(VO_4)_2](OH){\cdot}8.5H_2O$. *Z. Für Krist.* **2017**, *232*, 807–814. [CrossRef]
50. Cesbron, F. Nouvelles données sur la vanuralite. Existence de la méta-vanuralite. *Bull. Soc. Fr. Mineral. Cristallogr.* **1970**, *93*, 242–248.
51. Spano, T.L.; Olds, T.A.; Hall, S.M.; Van Gosen, B.S.; Kampf, A.R.; Burns, P.C.; Marty, J. Finchite, $Sr(UO_2)_2(V_2O_8){\cdot}5H_2O$, a new uranyl sorovanadate with the francevillite anion topology. *Am. Mineral.* **2023**, *108*, 383–388. [CrossRef]
52. Plášil, J.; Veselovský, F.; Hloušek, J.; Šák, M.; Sejkora, J.; Čejka, J.; Škácha, P.; Kasatkin, A.V. Mathesiusite, $K_5(UO_2)_4(SO_4)_4(VO_5)(H_2O)_4$, a new uranyl vanadate-sulfate from Jáchymov, Czech Republic. *Am. Mineral.* **2014**, *99*, 625–632. [CrossRef]
53. Kampf, A.R.; Plášil, J.; Nash, B.P.; Marty, J. Ammoniomathesiusite, a new uranyl sulfate-vanadate mineral from the Burro mine, San Miguel County, Colorado, USA. *Mineral. Mag.* **2019**, *83*, 115–121. [CrossRef]
54. Breithaupt, J.F.A. Mineralogische Studien. 2. Fritzscheït und Uranite überhaupt. *Berg-Und Huttenmann. Ztg.* **1865**, *24*, 302–303.
55. Hess, F.L. *Rauvite, a New Uranium-Vanadium Mineral*; U.S. Geological Survey Bulletin—Contributions to Economic Geology 750D; 1924; pp. 68–70. [CrossRef]
56. Hess, F.L.; Schaller, W.T. Pintadoite and uvanite, two new minerals from Utah: A preliminary note. *J. Wash. Acad. Sci.* **1914**, *4*, 576–579.
57. Suleimanov, E.V.; Somov, N.V.; Chuprunov, E.V.; Mayatskikh, E.F.; Depmeier, W.; Alekseev, E.V. A detailed study of the dehydration process in synthetic strelkinite, $Na[(UO_2)(VO_4)]{\cdot}nH_2O$ (n = 0, 1, 2). *Z. Kristallogr.* **2012**, *227*, 522–529. [CrossRef]
58. Dickens, P.G.; Stuttard, G.P.; Ball, R.G.J.; Powell, A.V.; Hull, S.; Patat, S. Powder Neutron Diffraction Study of the Mixed Uranium-Vanadium Oxides $Cs_2(UO_2)_2(V_2O_8)$ and UVO_5. *J. Mater. Chem.* **1992**, *2*, 161–166. [CrossRef]
59. Abraham, F.; Dion, C.; Tancret, N.; Saadi, M. $Ag_2(UO_2)_2V_2O_8$: A New Compound with the Carnotite Structure. Synthesis, Structure and Properties. *Adv. Mater. Res. Vols.* **1994**, *1–2*, 511–520. [CrossRef]
60. Wang, Y.; Yin, X.; Zhao, Y.; Gao, Y.; Chen, L.; Liu, Z.; Sheng, D.; Diwu, J.; Chai, Z.; Albrecht-Shmitt, T.E.; et al. Insertion of Trivalent Lanthanides into Uranyl Vanadate Layers and Frameworks. *Inorg. Chem.* **2015**, *54*, 8449–8455. [CrossRef]
61. Mer, A.; Obbade, S.; Devaux, P.; Abraham, F. Structural Evolution in the Rare-Earth Uranyl Vanadates $Ln_2[(UO_2)_2V_2O_8]_3{\cdot}nH_2O$, Singularity of the Lanthanum Compound, and Single-Crystal to Single-Crystal Partial Dehydration. *Cryst. Growth Des.* **2019**, *19*, 3305–3314. [CrossRef]
62. Duribreux, I.; Saadi, M.; Obbade, S.; Dion, C.; Abraham, F. Synthesis and crystal structure of two new uranyl oxychloro-vanadate layered compounds: $M_7(UO_2)_8(VO_4)_2O_8Cl$ with M=Rb, Cs. *J. Solid State Chem.* **2003**, *172*, 351–363. [CrossRef]
63. Dion, C.; Obbade, S.; Raekelboom, E.; Abraham, F. Synthesis, Crystal Structure, and Comparison of Two New Uranyl Vanadate Layered Compounds: $M_6(UO_2)_5(VO_4)_2O_5$ with M = Na, K. *J. Solid State Chem.* **2000**, *155*, 342–353. [CrossRef]
64. Obbade, S.; Dion, C.; Duvieubourg, L.; Saadi, M.; Abraham, F. Synthesis and crystal structure of a and b-Rb6U5V2O23, a new layered compound. *J. Solid State Chem.* **2003**, *173*, 1–12. [CrossRef]
65. Duribreux, I.; Dion, C.; Abraham, F. $CsUV_3O_{11}$, a New Uranyl Vanadate with a Layered Structure. *J. Solid State Chem.* **1999**, *146*, 258–265. [CrossRef]

66. Obbade, S.; Dion, C.; Saadi, M.; Abraham, F. Synthesis, crystal structure and electrical characterization of $Cs_4[(UO_2)_2(V_2O_7)O_2]$, a uranyl divanadate with chains of corner-sharing uranyl square bipyramids. *J. Solid State Chem.* **2004**, *177*, 1567–1574. [CrossRef]
67. Chong, S.; Aksenov, S.M.; Dal Bo, F.; Perry, S.N.; Dimakopoulou, F.; Burns, P.C. Framework Polymorphism and Modular Crystal Structures of Uranyl Vanadates of Divalent Cations: Synthesis and Characterization of $M(UO_2)(V_2O_7)$(M = Ca, Sr) and $Sr_3(UO_2)(V_2O_7)_2$. *Z. Anorg. Allg. Chem.* **2019**, *645*, 981–987. [CrossRef]
68. Mer, A.; Obbade, S.; Rivenet, M.; Renard, C.; Abraham, F. $[La(UO_2)V_2O_7][(UO_2)(VO_4)]$ the first lanthanum uranyl-vanadate with structure built from two types of sheets based upon the uranophane anion-topology. *J. Solid State Chem.* **2012**, *185*, 180–186. [CrossRef]
69. Saadi, M.; Dion, C.; Abraham, F. Synthesis and Crystal Structure of the Pentahydrated Uranyl Orthovanadate $(UO_2)_3(VO_4)_2{\cdot}5H_2O$, Precursor for the New $(UO_2)_3(VO_4)_2$ Uranyl-Vanadate. *J. Solid State Chem.* **2000**, *150*, 72–80. [CrossRef]
70. Tancret, N.; Obbade, S.; Abraham, F. Ab initio Structure Determination of Uranyl Divanadate $(UO_2)_2V_2O_7$ from Powder X-Ray Diffraction Data. *Eur. J. Solid State Inorg. Chem.* **1995**, *32*, 195–207. [CrossRef]
71. Obbade, S.; Dion, C.; Saadi, M.; Yagoubi, S.; Abraham, F. $Pb(UO_2)(V_2O_7)$, a novel lead uranyl divanadate. *J. Solid State Chem.* **2004**, *177*, 3909–3917. [CrossRef]
72. Obbade, S.; Duvieubourg, L.; Dion, C.; Abraham, F. Three-dimensional framework of uranium-centered polyhedra with non-intersecting channels in the uranyl oxy-vanadates $A_2(UO_2)_3(VO_4)_2O$ (A = Li, Na). *J. Solid State Chem.* **2007**, *180*, 866–872. [CrossRef]
73. Obbade, S.; Dion, C.; Rivenet, M.; Abraham, F. A novel open-framework with non-crossing channels in the uranyl vanadates $A(UO_2)_4(VO_4)_3$ (A=Li, Na). *J. Solid State Chem.* **2004**, *177*, 2058–2067. [CrossRef]
74. Obbade, S.; Renard, C.; Abraham, F. New open-framework in the uranyl vanadates $A_3(UO_2)_7(VO_4)_5O$(A = Li, Ag) with intergrowth structure between $A(UO_2)_4(VO_4)_3$ and $A_2(UO_2)_3(VO_4)_2O$. *J. Solid State Chem.* **2009**, *182*, 413–420. [CrossRef]
75. Shvareva, T.Y.; Beitz, J.V.; Duin, E.C.; Albrecht-Schmitt, T.E. Polar Open-Framework Structure, Optical Properties, and Electron Paramagnetic Resonance of the Mixed-Metal Uranyl Phosphate $Cs_2[UO_2(VO_2)_2(PO_4)_2]{\cdot}0.59H_2O$. *Chem. Mater.* **2005**, *17*, 6219–6222. [CrossRef]
76. Shvareva, T.Y.; Skanthakumar, S.; Soderholm, L.; Clearfield, A.; Albrecht-Schmitt, T.E. Cs^+-Selective Ion Exchange and Magnetic Ordering in a Three-Dimensional Framework Uranyl Vanadium(IV) Phosphate. *Chem. Mater.* **2007**, *19*, 132–134. [CrossRef]
77. Sykora, R.E.; Albrecht-Schmitt, T.E. Self-Assembly of a Polar Open-Framework Uranyl Vanadyl Hexaoxoiodate(VII) Constructed Entirely from Distorted Octahedral Building Units in the First Uranium Hexaoxoiodate: $K_2[(UO_2)_2(VO)_2(IO_6)_2O]{\cdot}H_2O$. *Inorg. Chem.* **2003**, *42*, 2179. [CrossRef] [PubMed]
78. Rivenet, M.; Vigier, N.; Roussel, P.; Abraham, F. Hydrothermal synthesis, structure and thermal stability of diamine templated layered uranyl-vanadates. *J. Solid State Chem.* **2007**, *180*, 713–724. [CrossRef]
79. Jouffret, L.; Shao, Z.; Rivenet, M.; Abraham, F. New three-dimensional inorganic frameworks based on the uranophane-type sheet in monoamine templated uranyl-vanadates. *J. Solid State Chem.* **2010**, *183*, 2290–2297. [CrossRef]
80. Jouffret, L.; Rivenet, M.; Abraham, F. A new series of pillared uranyl-vanadates based on uranophane-type sheets in the uranium-vanadium-linear alkyl diamine systems. *J. Solid State Chem.* **2010**, *183*, 84–92. [CrossRef]
81. Senchyk, G.A.; Wylie, E.M.; Prizio, S.; Szymanowski, J.E.S.; Sigmon, G.E.; Burns, P.C. Hybrid uranyl–vanadium nano-wheels. *Chem. Commun.* **2015**, *51*, 10134–10137. [CrossRef] [PubMed]
82. Hazen, R.M.; Ewing, R.C.; Sverjensky, D.A. Evolution of uranium and thorium minerals. *Am. Mineral.* **2009**, *94*, 1293–1311. [CrossRef]
83. Fischer, R.P. Uranium-bearing sandstone deposits of the Colorado Plateau. *Econ. Geol.* **1950**, *45*, 1–11. [CrossRef]
84. Weeks, A.D.; Thompson, M.E. Identification and occurrence of uranium and vanadium minerals from the Colorado Plateaus: Mineral associations and distribution of types of ore. *Bull. United States Geol. Surv.* **1954**, *1009-B*, 18–22.
85. Jones, W. The structure and properties of pillared clays. *Catal. Today* **1988**, *2*, 357–367. [CrossRef]
86. Vicente, M.A.; Gil, A.; Bergaya, F. Pillared Clays and Clay Minerals. In *Developments in Clay Science*, 2nd ed.; Bergaya, F., Lagaly, G., Eds.; Elsevier Ltd.: Amsterdam, The Netherlands, 2013. [CrossRef]
87. Durova, E.V.; Kuporev, I.V.; Gurzhiy, V.V. Organically Templated Uranyl Sulfates and Selenates: Structural Complexity and Crystal Chemical Restrictions for Isotypic Compounds Formation. *Int. J. Mol. Sci.* **2023**, *24*, 13020. [CrossRef]
88. Krivovichev, S.V.; Gurzhii, V.V.; Tananaev, I.G.; Myasoedov, B.F. Topology of Inorganic Complexes as a Function of Amine Molecular Structure in Layered Uranyl Selenates. *Dokl. Phys. Chem.* **2006**, *409*, 228–232. [CrossRef]

89. Krivovichev, S.V.; Gurzhiy, V.V.; Tananaev, I.G.; Myasoedov, B.F. Amine-Templated Uranyl Selenates with Chiral $[(UO_2)_2(SeO_4)_3(H_2O)]^{2-}$ Layers: Topology, Isomerism, Structural Relationships. *Z. Kristallogr. Cryst. Mater.* **2009**, *224*, 316–324. [CrossRef]
90. Tschauner, O.; Bermanec, M. Crystal Structure Complexity and Approximate Limits of Possible Crystal Structures Based on Symmetry-Normalized Volumes. *Materials* **2024**, *17*, 2618. [CrossRef]